

Electromagnetic moments of the τ lepton with CMS

Cécile Caillol (CERN), on behalf of the CMS experiment

NuFact, September 2024

CMS closes in on tau g-2

19 March 2024

A report from the CMS experiment



The CMS experiment. Credit: J Hosan / OPEN-PHO-LIFE-2019-022-5

The CMS collaboration [has reported](#) the first observation of $\gamma\gamma \rightarrow \tau\tau$ in pp collisions. The results set a new benchmark for the tau lepton's magnetic moment, surpassing previous constraints and paving the way for studies probing new physics.

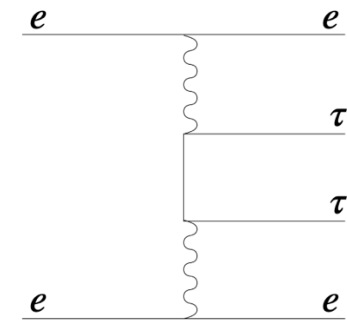
τ $g-2$ less well known than e and μ $g-2$...

- Tau leptons have a **very short lifetime** and cannot be stored in storage rings

$$\mu_{\tau}/(e\hbar/2m_{\tau})-1 = (g_{\tau}-2)/2$$

For a theoretical calculation $[(g_{\tau}-2)/2 = 117\,721(5) \times 10^{-8}]$, see EIDELMAN 07.

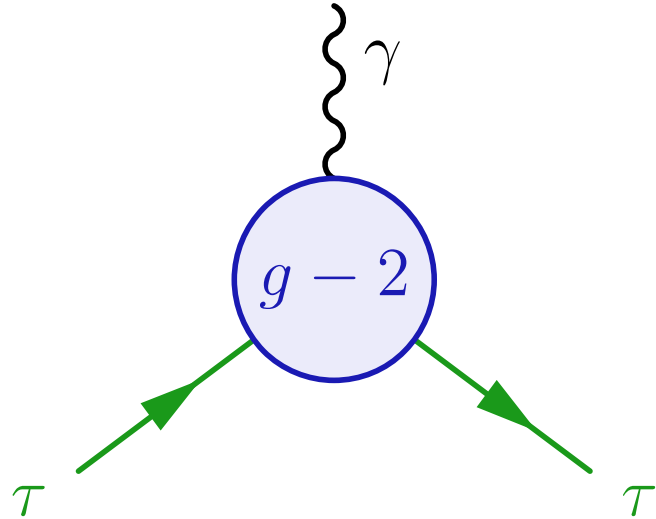
| VALUE | CL% | DOCUMENT ID | TECN | COMMENT |
|--|-----|-----------------------|----------|--|
| > -0.052 and < 0.013 (CL = 95%) OUR LIMIT | | | | |
| > -0.052 and < 0.013 | 95 | ¹ ABDALLAH | 04K DLPH | $e^+e^- \rightarrow e^+e^-\tau^+\tau^-$ at LEP2 |



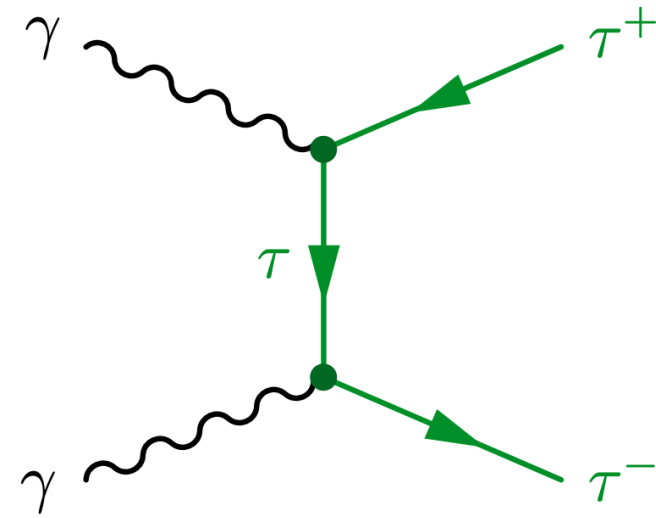
- Limit from PDG dates back 20 years (LEP) and is about 20 times the Schwinger term
- Many **orders of magnitude less precise** than e and μ $g-2$ measurements!
- If BSM effects scale with the squared lepton mass (m_{ℓ}^2), deviations from the SM could be 280 times larger than for a_{μ}

At the LHC: τ moments from $\gamma\gamma \rightarrow \tau\tau$ events

- τ $g-2$ can be indirectly probed from $\gamma\tau\tau$ vertex



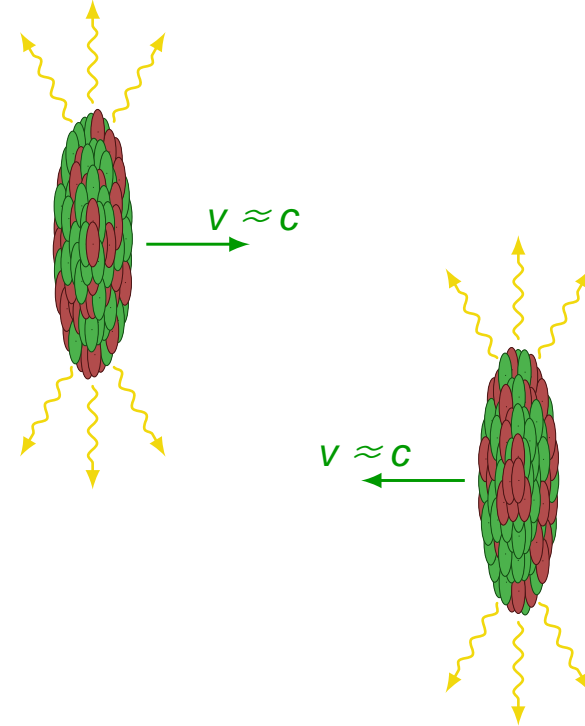
- Photon-induced processes: $\gamma\gamma \rightarrow \tau\tau$ includes 2 $\gamma\tau\tau$ vertices



- Constraints on τ electromagnetic moments from effective field theory approach (SMEFT) based on (differential) cross section measurement of $\gamma\gamma \rightarrow \tau\tau$

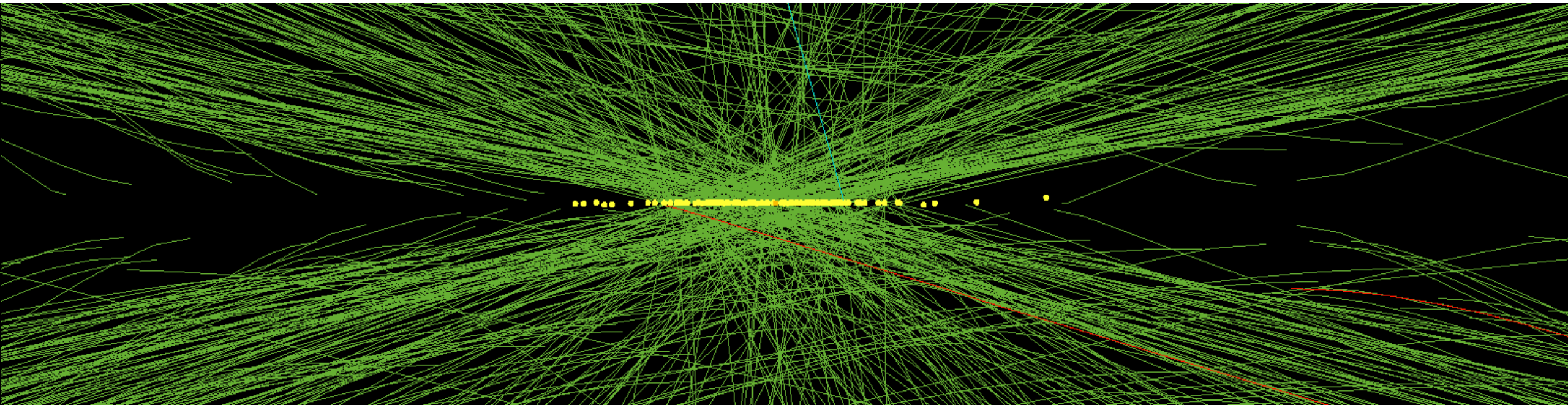
Photon-induced processes at the LHC

- Two charged particles (e.g. protons or ions) passing each other at relativistic velocities generate intense electromagnetic fields → **photon-photon collisions** can happen
- Typically study “head-on” collisions but rare photon-induced processes can be studied in ultraperipheral collisions
- Protons losing some of their energy to the photons are slightly deflected
- **Cross section proportional to Z^4** → huge enhancement of photon-induced processes in Pb-Pb ($Z = 82$) runs compared to pp runs



pp collisions with track counting

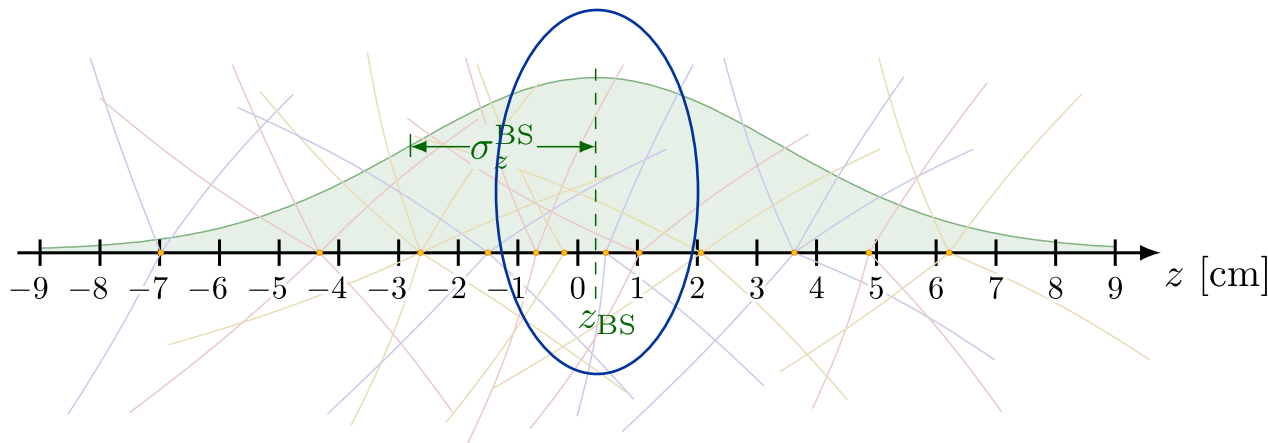
- If energy too low for protons to be in PPS acceptance, the only way to identify photon-induced processes is through a **vertex with very little track activity**
- Photon-induced processes are exceptionally clean but proton-proton collisions are incredibly busy
→ challenging to identify a vertex among all pileup interactions



Counting tracks

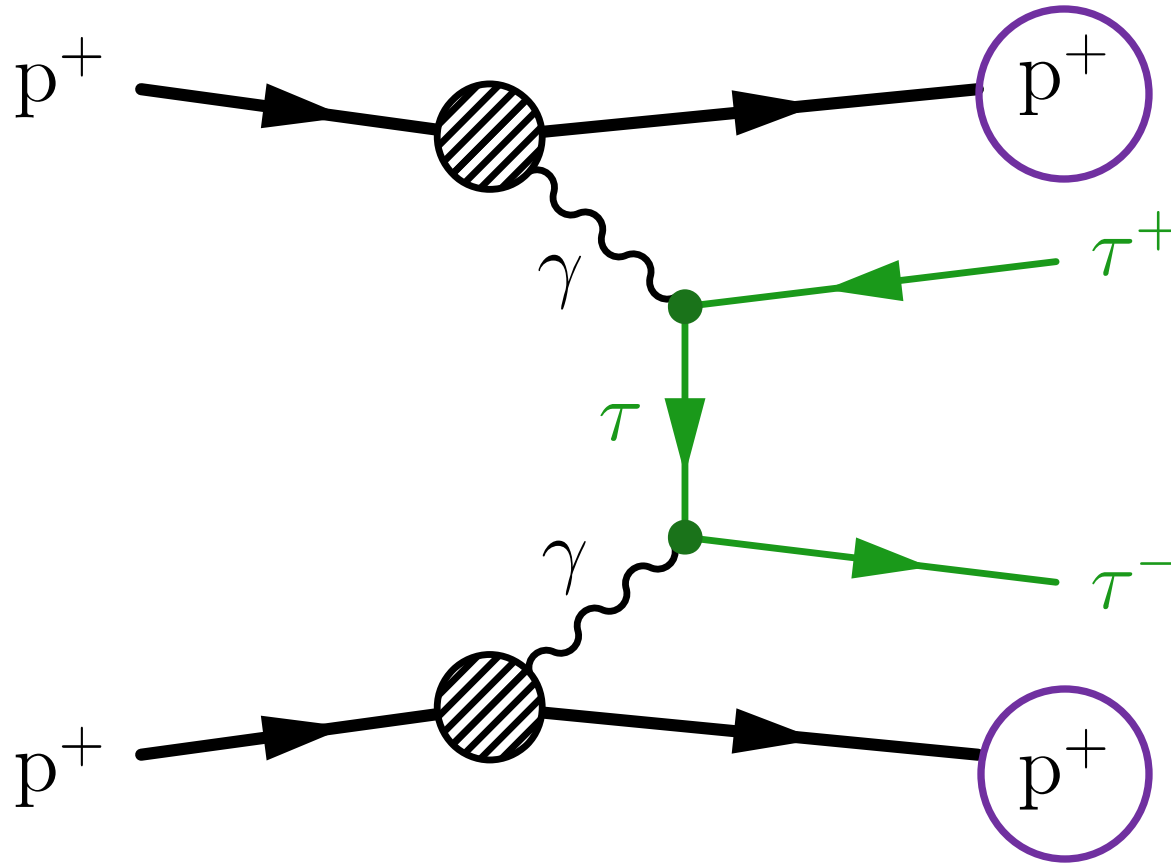
- Define **z position of di-tau vertex** as average z position of selected tau leptons
- Define **N_{tracks}** as the number of tracks
 - with $p_{\tau} > 0.5$ GeV and $|\eta| < 2.5$
 - within a window of **0.1 cm** around the di-tau vertex
 - Excluding tracks from tau leptons

Simulations cannot model track multiplicity accurately → correct them using data



- About 30% of the windows at the center of the beamspot do not contain any pileup track

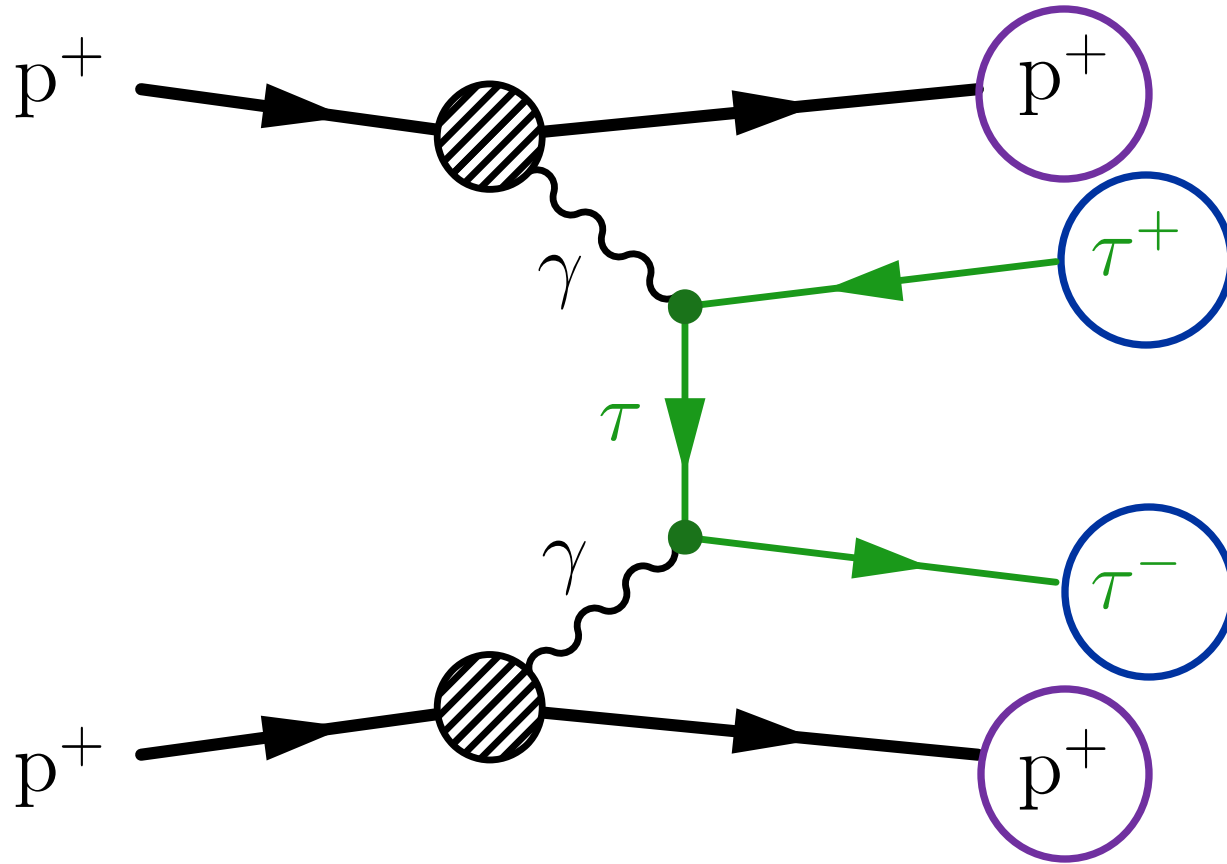
Signature



- 2 diffracted protons
- Could be reconstructed in PPS if $m_{\tau\tau} \gtrsim 350 \text{ GeV} \rightarrow$ low signal acceptance
- Decided not to require diffracted protons in the analysis

Elastic process, protons do not dissociate

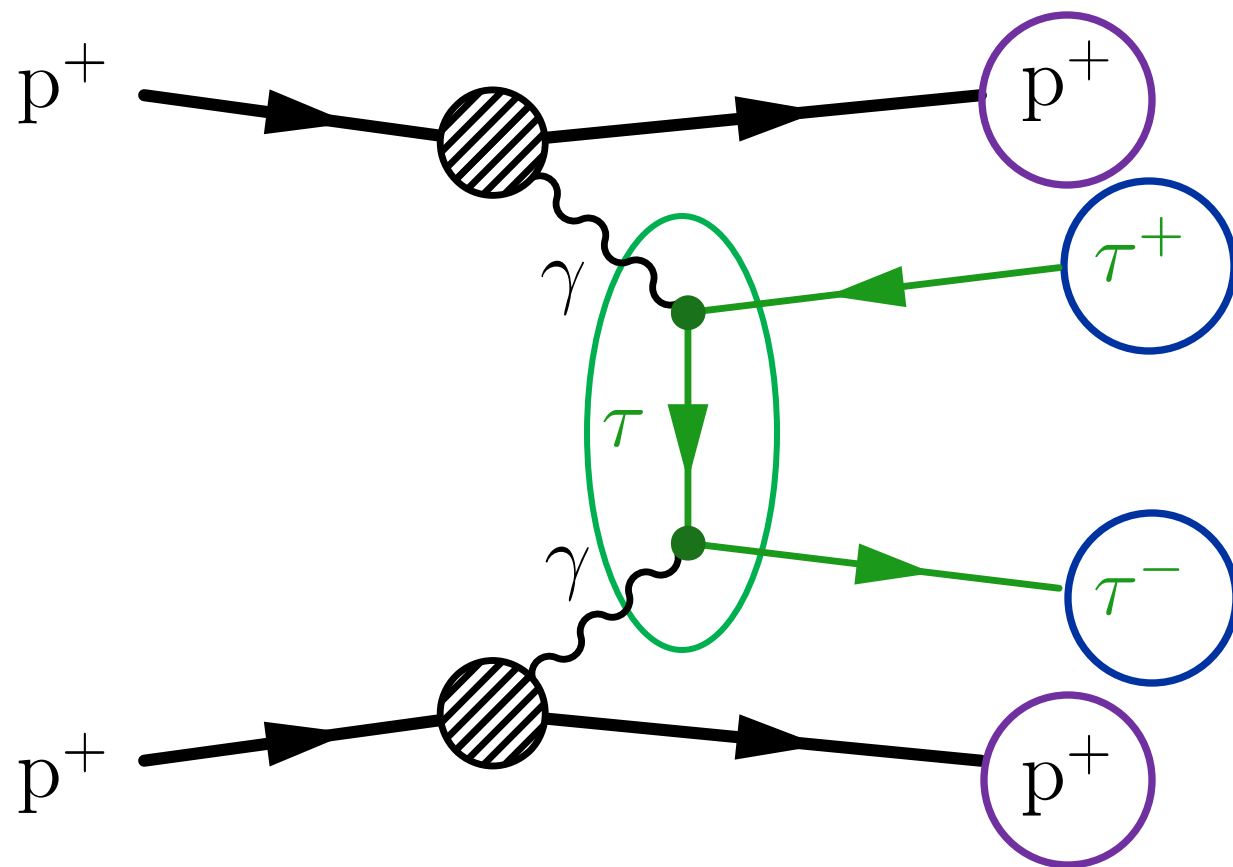
Signature



- 2 diffracted protons
- 2 back-to-back OS τ leptons
 - Acoplanarity $A = 1 - \frac{|\Delta\phi|}{\pi} \approx 0$

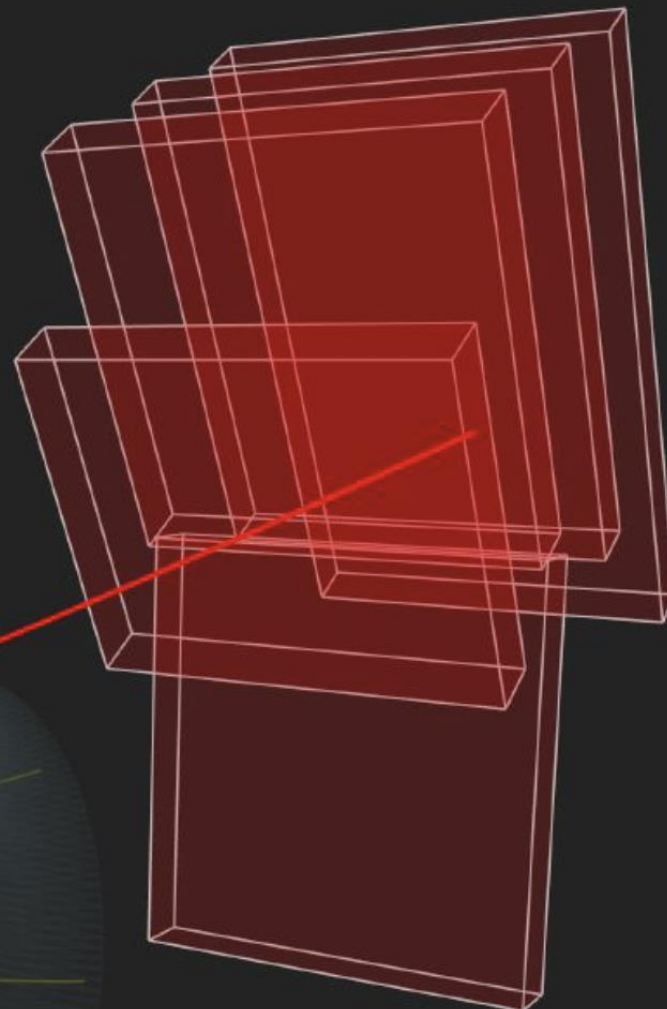
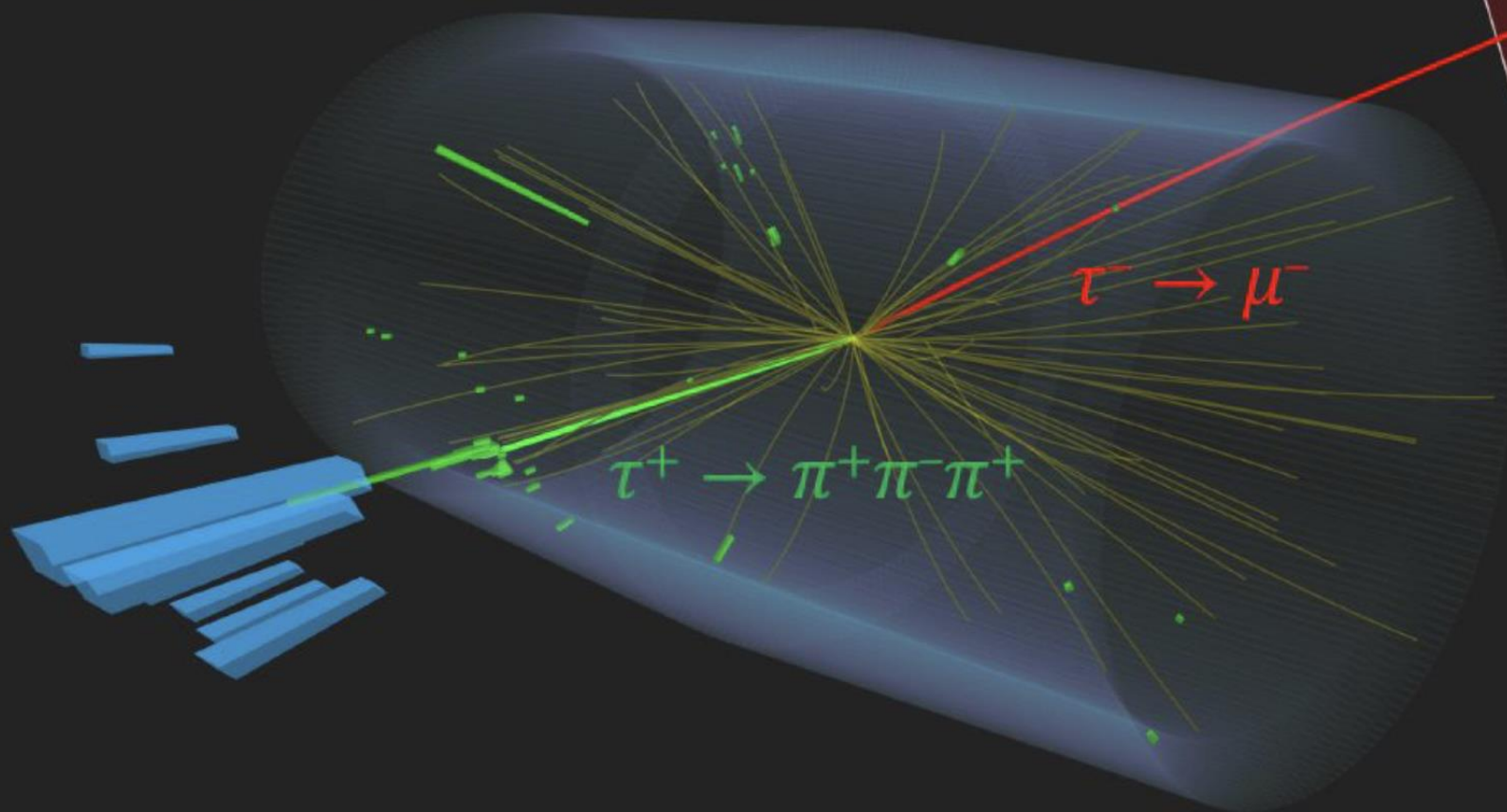
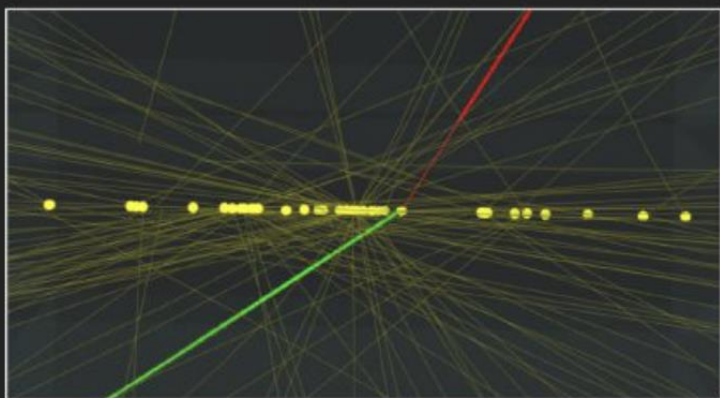
Elastic process, protons do not dissociate

Signature

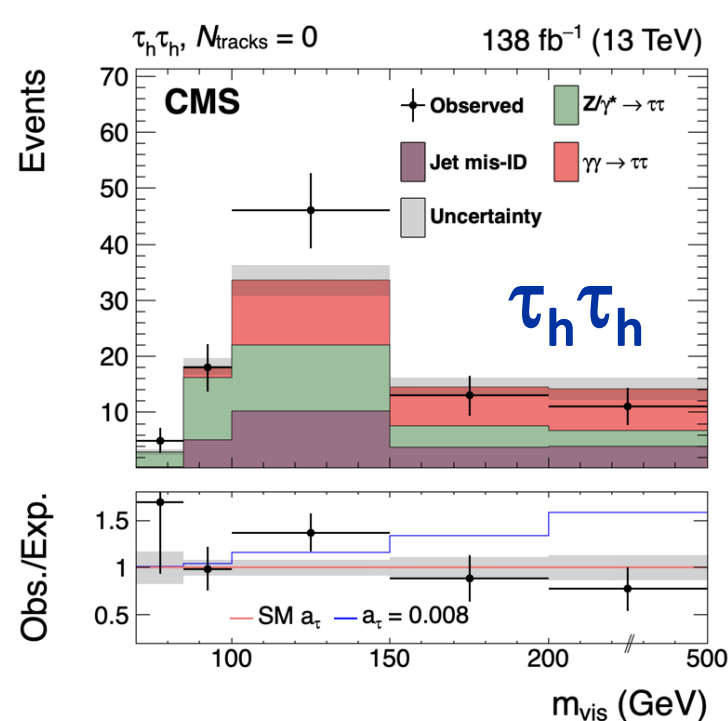
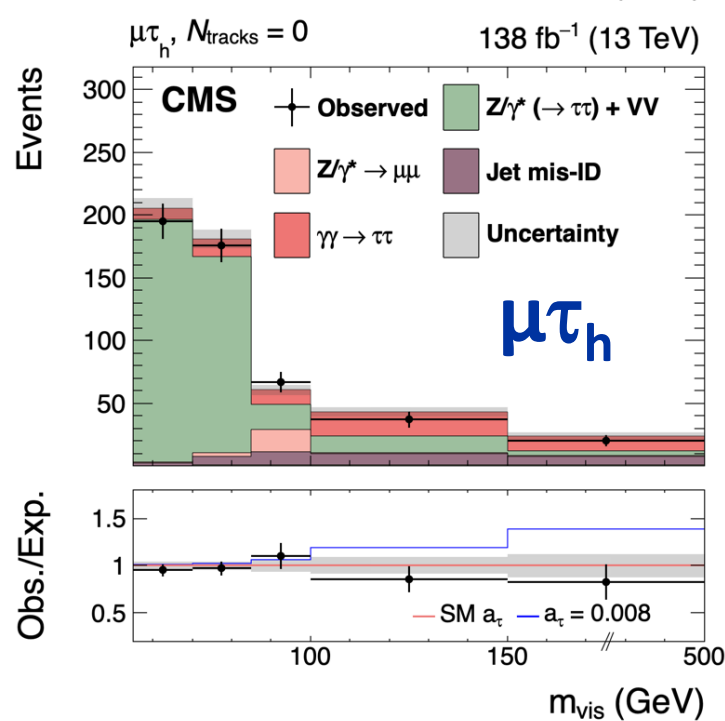
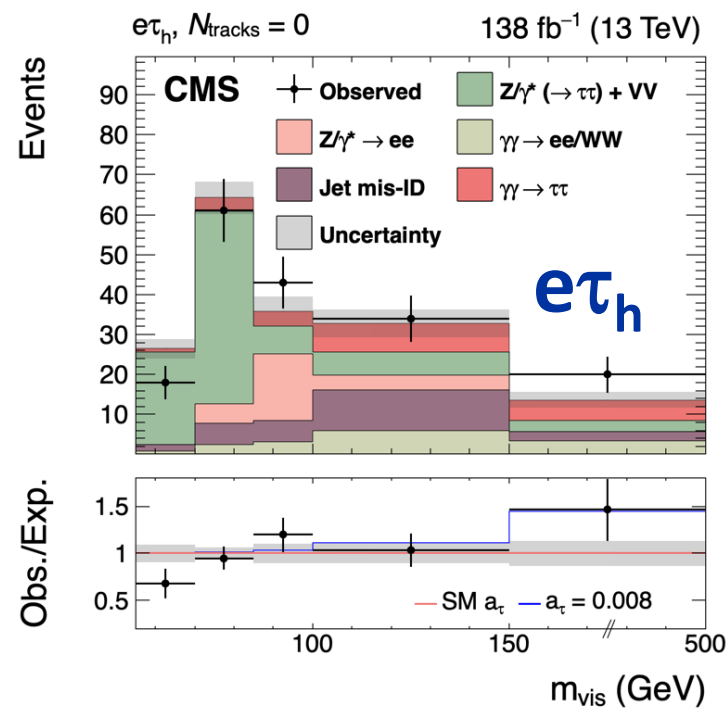
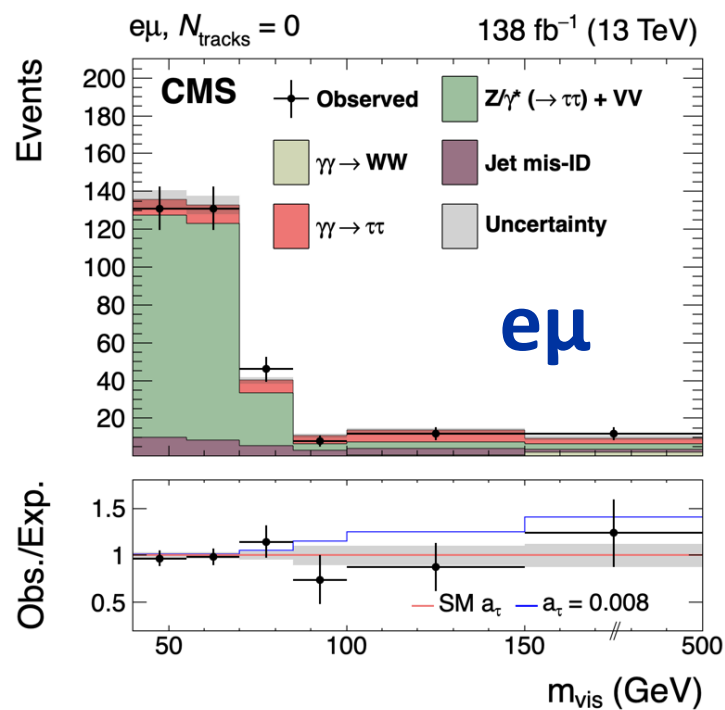


- 2 diffracted protons
- 2 back-to-back OS τ leptons
- No hadronic activity close to the di- τ vertex
 - $N_{\text{tracks}} = 0$

Elastic process, protons do not dissociate



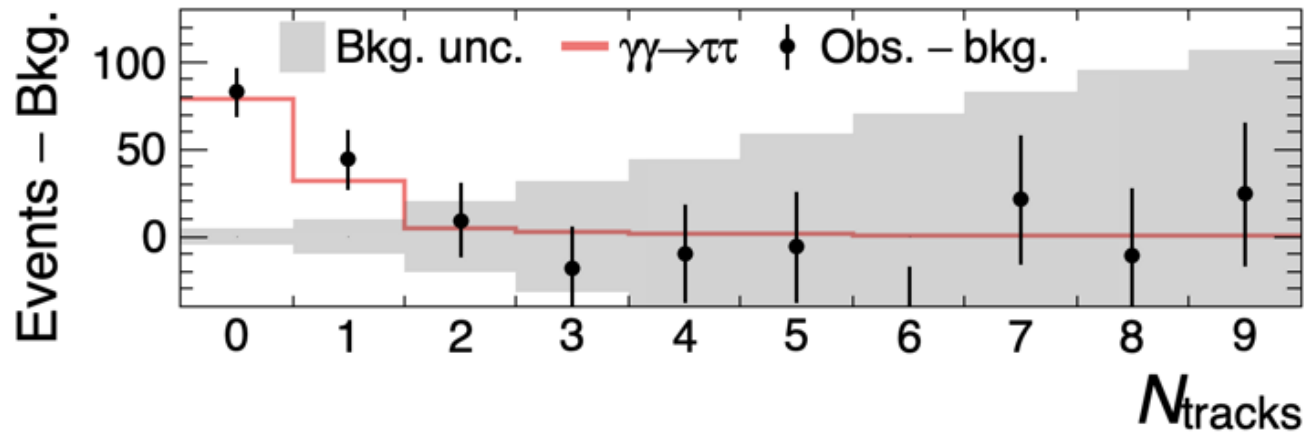
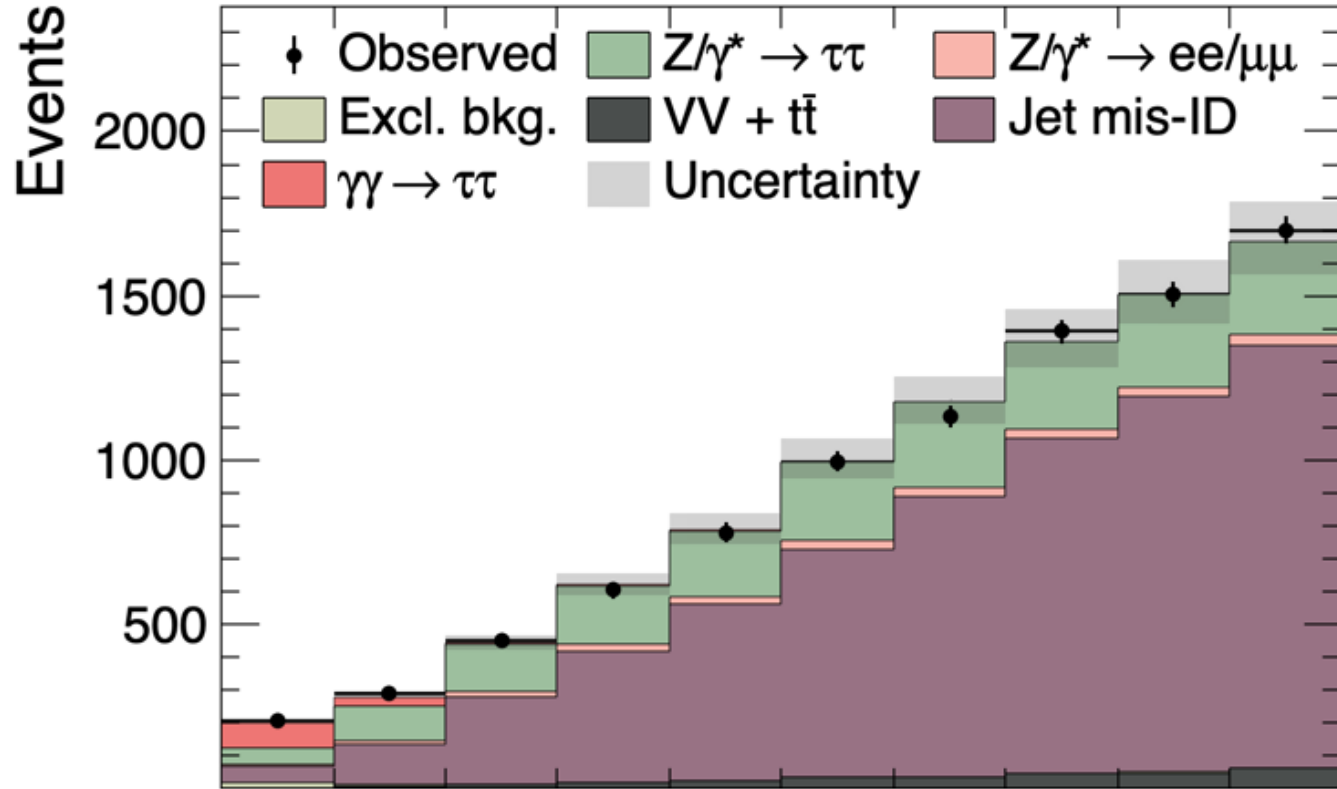
$N_{\text{tracks}} = 0$



- m_{vis} distributions in the different final states after the maximum likelihood fit, assuming SM a_τ and d_τ
- **Signal visible in high m_{vis} bins**
- **5.3 σ observed, 6.5 σ expected**
- **First observation of $\gamma\gamma \rightarrow \tau\tau$ in pp collisions**

CMS

138 fb⁻¹ (13 TeV)



- N_{tracks} distribution for events with $m_{\text{vis}} > 100$ GeV
- We can model well the N_{tracks} distribution for backgrounds
- The signal is seen as an excess of events at very low N_{tracks}

Constraining τ g-2 with an effective field theory

- Two dimension-6 operators modify a_τ at tree-level in the SMEFT:

$$\mathcal{L}_{\text{BSM}} = \frac{C_{\tau B}}{\Lambda^2} \bar{L}_L \sigma^{\mu\nu} \tau_R H B_{\mu\nu} + \frac{C_{\tau W}}{\Lambda^2} \bar{L}_L \sigma^{\mu\nu} \tau_R \sigma^i H W_{\mu\nu}^i + \text{h.c.}$$

- BSM contributions to a_τ :

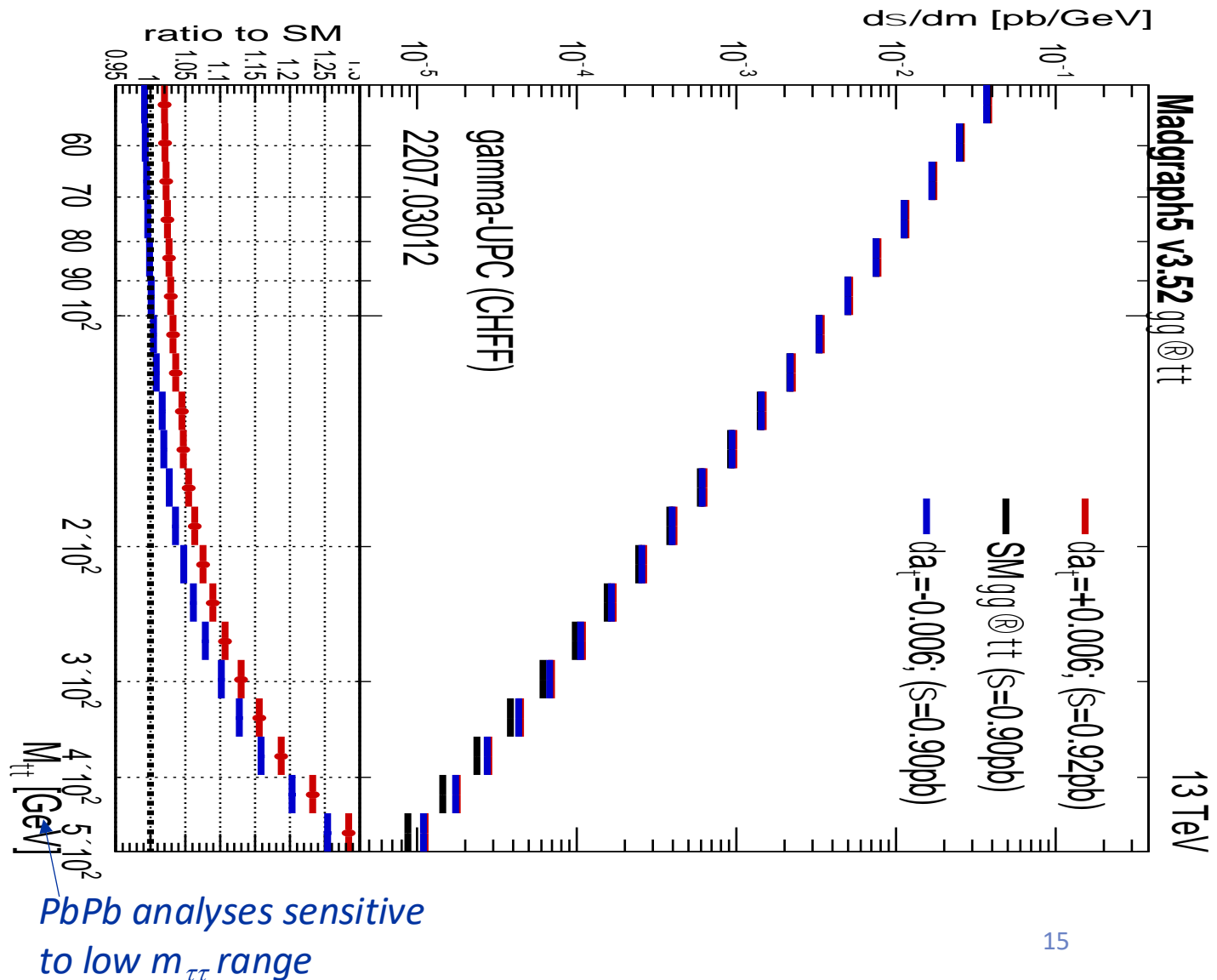
SMEFT-sim_general alphaScheme_UFO

$$\delta a_\tau = \frac{2m_\tau}{e} \frac{\sqrt{2}v}{\Lambda^2} \text{Re} [C_{\tau\gamma}]$$

where $C_{\tau\gamma} = (\cos\theta_W C_{\tau B} - \sin\theta_W C_{\tau W})$

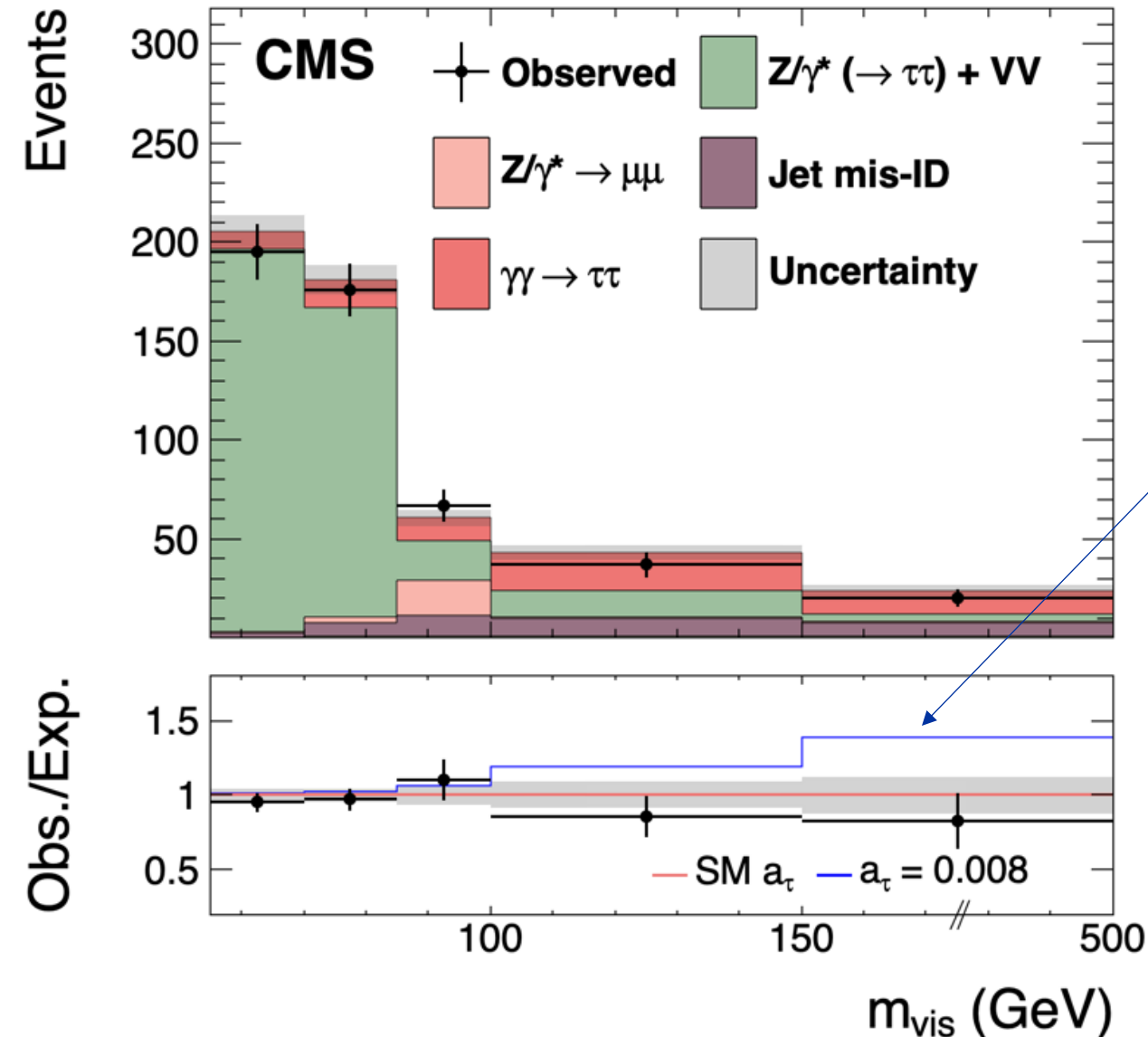
How BSM physics in a_τ affects $\gamma\gamma \rightarrow \tau\tau$

- At large $m_{\tau\tau}$, $\gamma\gamma \rightarrow \tau\tau$ cross section increases with both positive and negative variations to a_τ
- The effect grows with $m_{\tau\tau}$
- We can constrain a_τ by looking at the yield and $m_{\tau\tau}$ distribution of the $\gamma\gamma \rightarrow \tau\tau$ process
- Expect better BSM sensitivity than with Pb-Pb runs because of higher $m_{\tau\tau}$ range probed



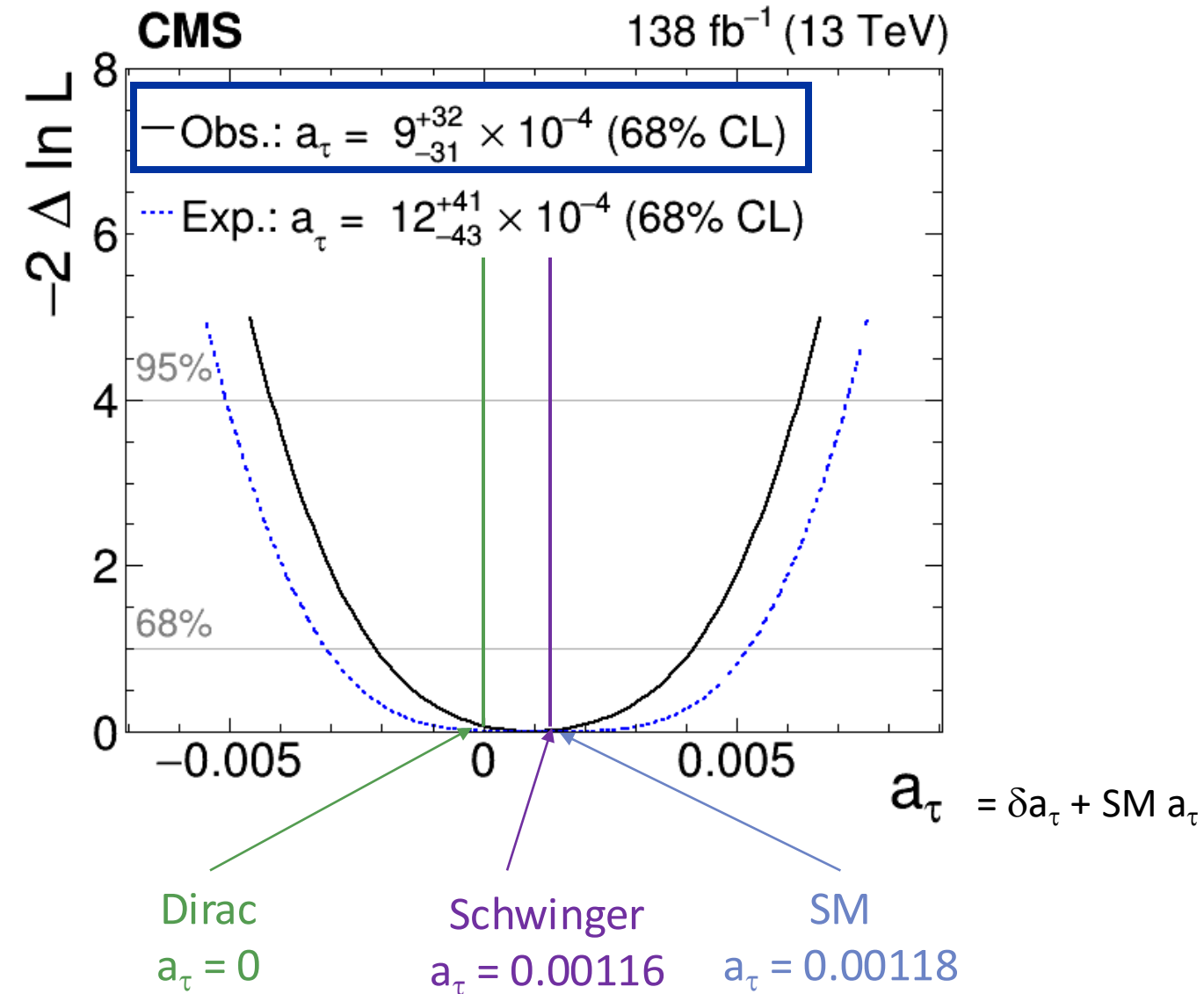
How it translates in this analysis

$\mu\tau_h, N_{\text{tracks}} = 0$ 138 fb⁻¹ (13 TeV)



- Changing a_τ from its SM value modifies the $\gamma\gamma \rightarrow \tau\tau$ prediction
- Differences between SM and BSM a_τ scenarios increase with m_{vis}
- a_τ can be constrained from the same m_{vis} distributions used to observe $\gamma\gamma \rightarrow \tau\tau$

Extracting a_τ



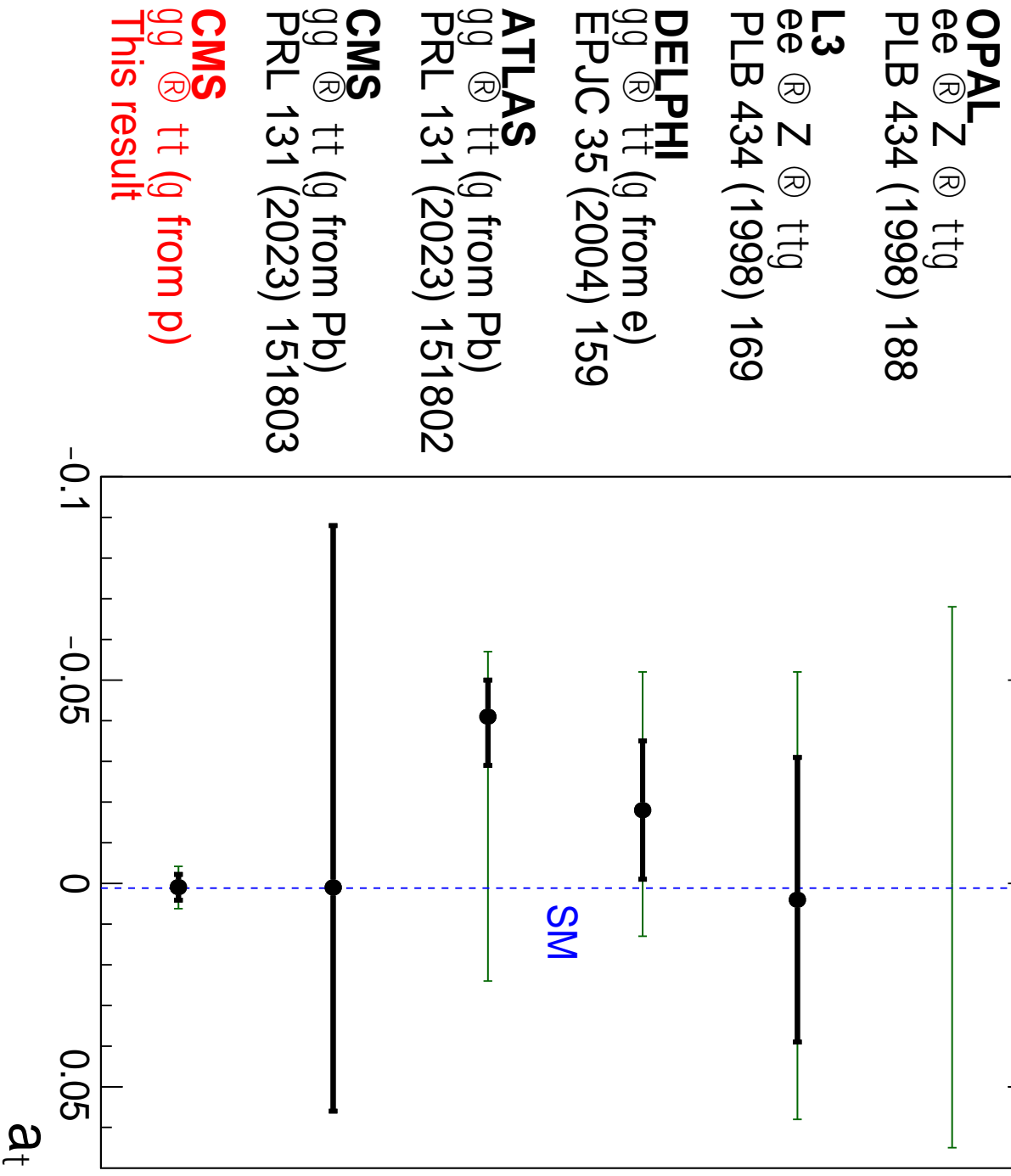
1 σ uncertainty of 0.003

Only 3 times the Schwinger term!

CMS

138 fb⁻¹ (13 TeV)

- Observed — 68% CL — 95% CL



Comparing to previous results

Large improvement
over LEP and LHC Pb-Pb

Conclusion

- **The LHC is also a high energy photon collider**
- The CMS experiment can indirectly probe the τ g-2 in photon-induced collisions ($\gamma\gamma \rightarrow \tau\tau$) both in PbPb and pp runs
- **The CMS Collaboration has observed, for the first time, $\gamma\gamma \rightarrow \tau\tau$ events in pp runs**
- These events were used to constrain the tau g-2: $-0.0042 < a_\tau < 0.0062$ at 95% CL, **improving previous constraints on tau g-2 by almost an order of magnitude**

Backup

The precision journey has just started...

DELPHI

CMS pp

OPAL

Approaching the

Pb-Pb LHC

Schwinger term!

More precision needed to
probe BSM effects scaling
with m_ℓ^2 ...

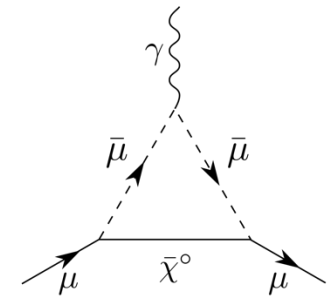
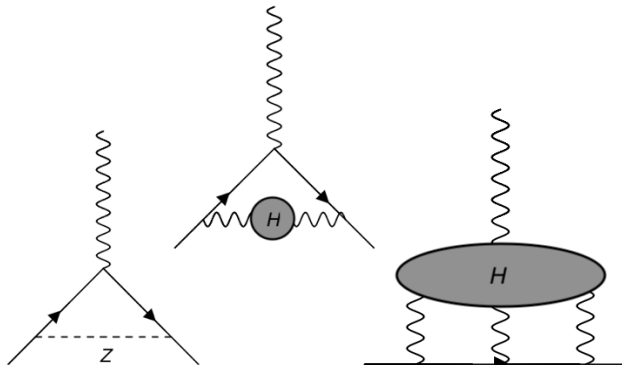
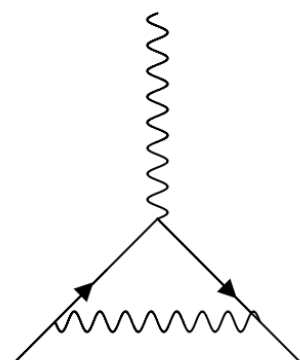
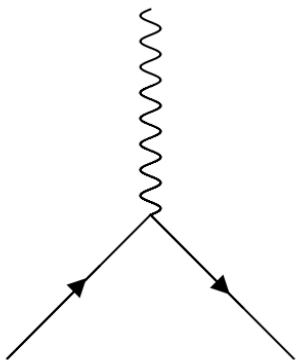


Dirac

Schwinger term

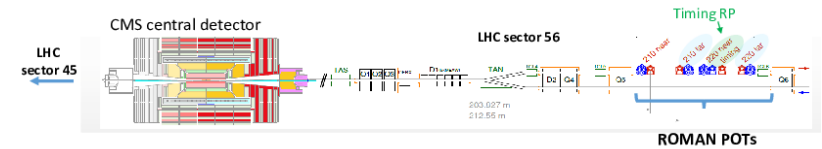
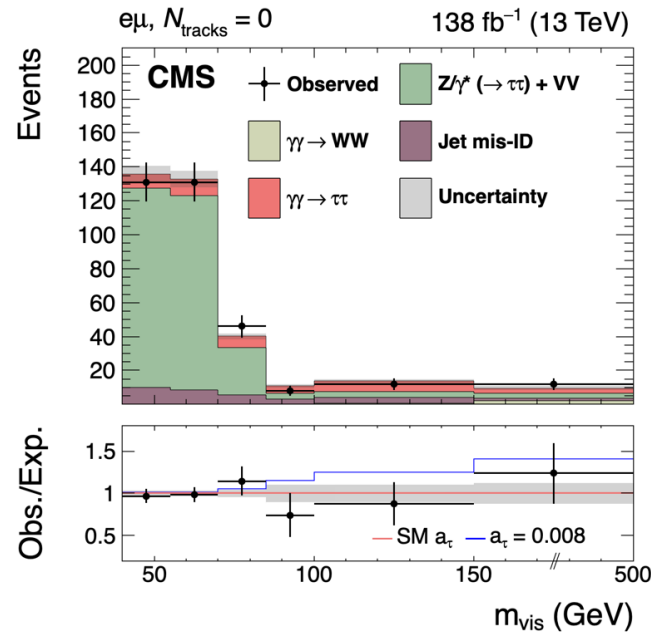
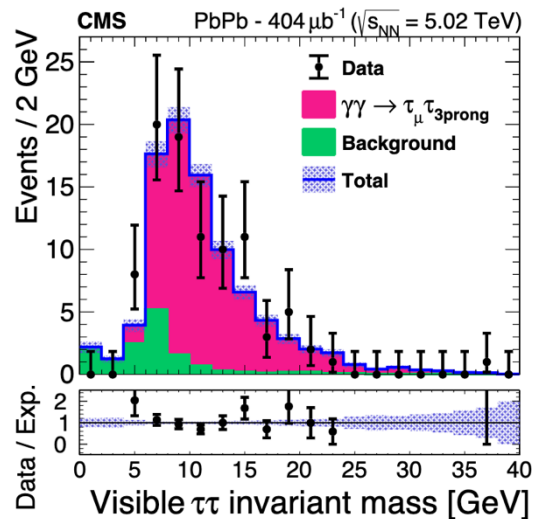
Higher-order corrections

BSM effects?



... and CMS will be a part of it

- Heavy ion runs
- pp runs with track counting
- pp runs with proton tagging



PPS approved for Run-4

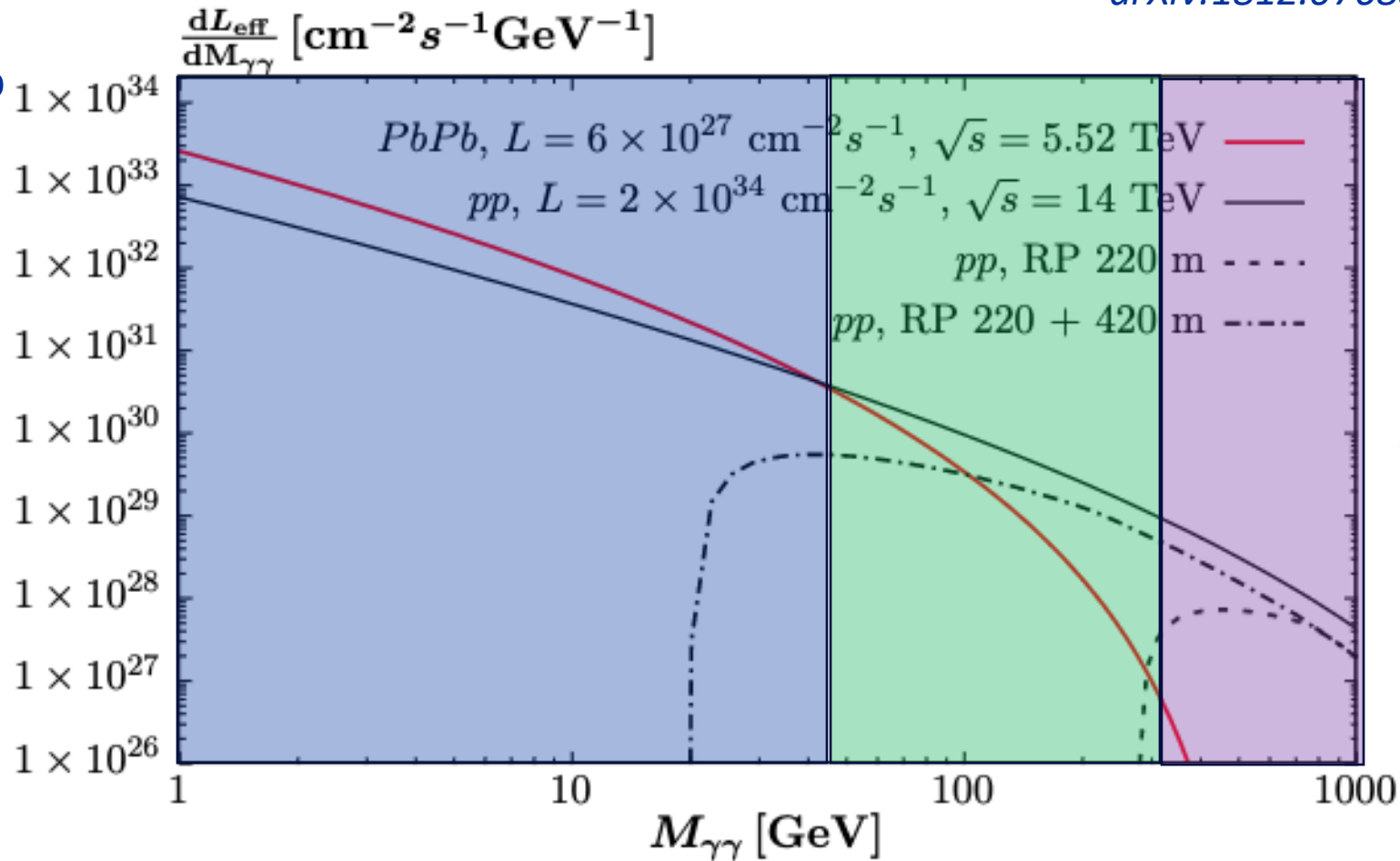


The majority of CMS data has not been collected yet. Exciting complementary approaches for upcoming Runs!

The LHC is (also) a photon collider

arXiv:1812.07688

At low masses, PbPb runs have the largest effective $\gamma\gamma$ luminosity

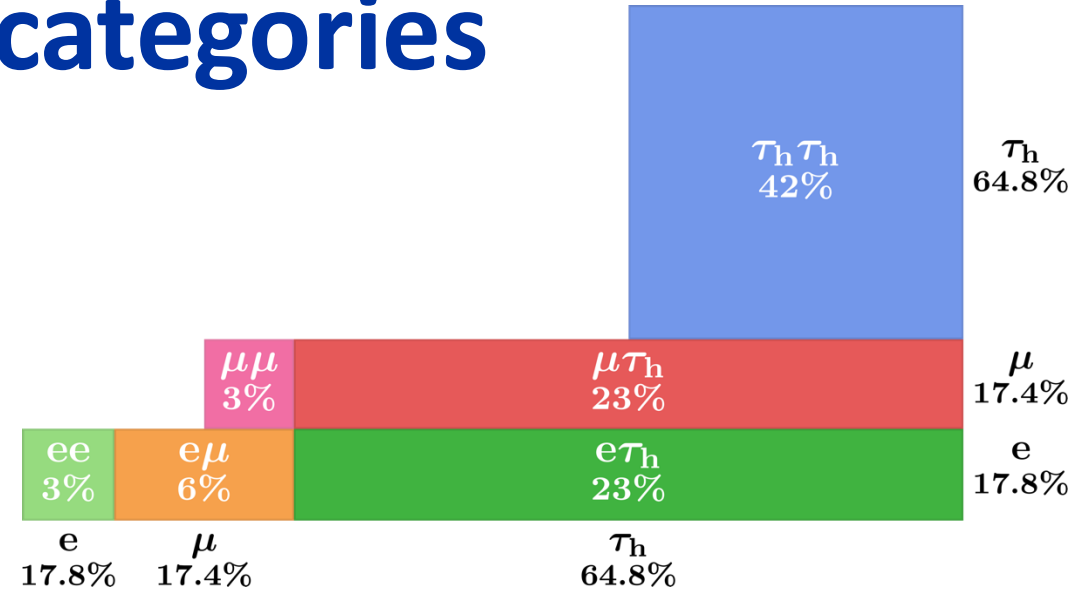


At very high masses, diffracted protons can be tagged by forward detectors

At intermediate masses, pp takes over but need to handle pileup

Final states and categories

- 4 di-tau final states: $e\mu$, $e\tau_h$, $\mu\tau_h$, $\tau_h\tau_h$



- In each di-tau final state, 2 signal regions: $N_{\text{tracks}} = 0$ or 1
 - $N_{\text{tracks}} = 0$: ~50% of the signal, inclusive backgrounds reduced by $O(10^3)$
 - $N_{\text{tracks}} = 1$: ~25% of the signal, larger background
- Dimuon control region to derive corrections to the simulations

Dominant backgrounds

- $Z/\gamma^* \rightarrow \tau\tau$ (Drell-Yan)

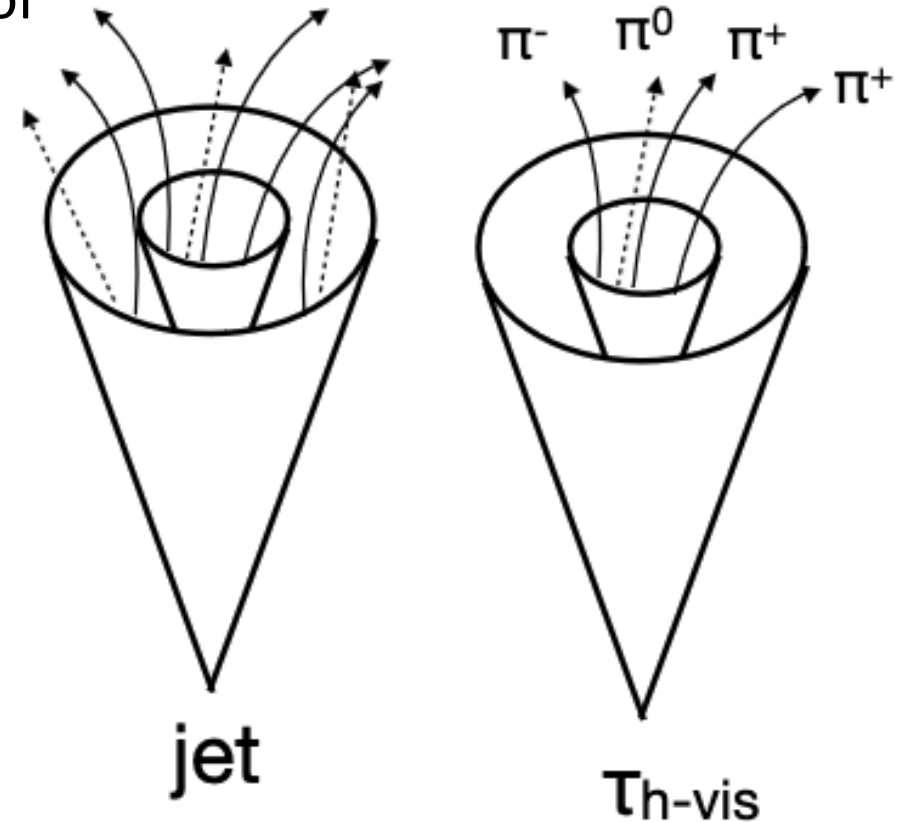
- Same final state as the signal but more tracks at the vertex (from hard scattering)
- Resonant ditau production \rightarrow ditau mass peaks at Z mass
- Taus are rather back-to-back (low acoplanarity) but less so than for the signal
- Estimated from simulation with data-driven corrections

- Jet mis-ID (QCD, W+jets, ...):

- When a jet is misreconstructed as a tau
- Data-driven estimation (no reliable MC prediction)
- Nonresonant, mass distribution similar to that of the signal

Jets misidentified as τ_h

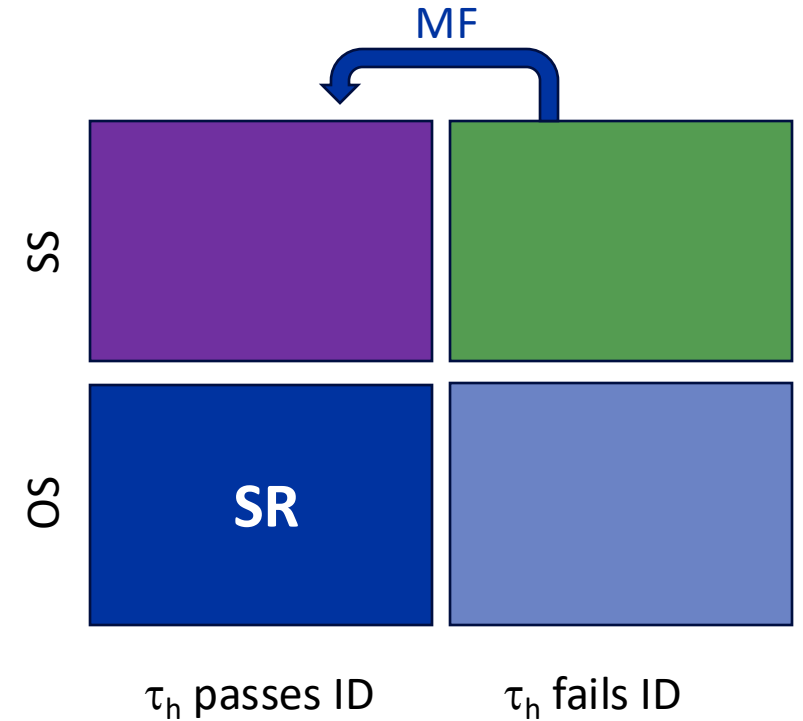
- Hadronically decaying taus (τ_h) are reconstructed as 1 or 3 tracks with energy deposits in the calorimeters
- Typically look like quark- and gluon-jets
- Main handles to separate τ_h and jets:
 - τ_h are **more isolated** (less activity around)
 - τ_h are **slightly displaced** (from τ lifetime)
- Information used in a neural net



Jet \rightarrow τ_h mis-ID background (1)

- Measure "mis-ID factor", MF, for jets as

$$MF = \frac{N(\text{jets passing nominal } \tau_h \text{ ID})}{N(\text{jets failing nominal } \tau_h \text{ ID but passing very loose } \tau_h \text{ ID})}$$



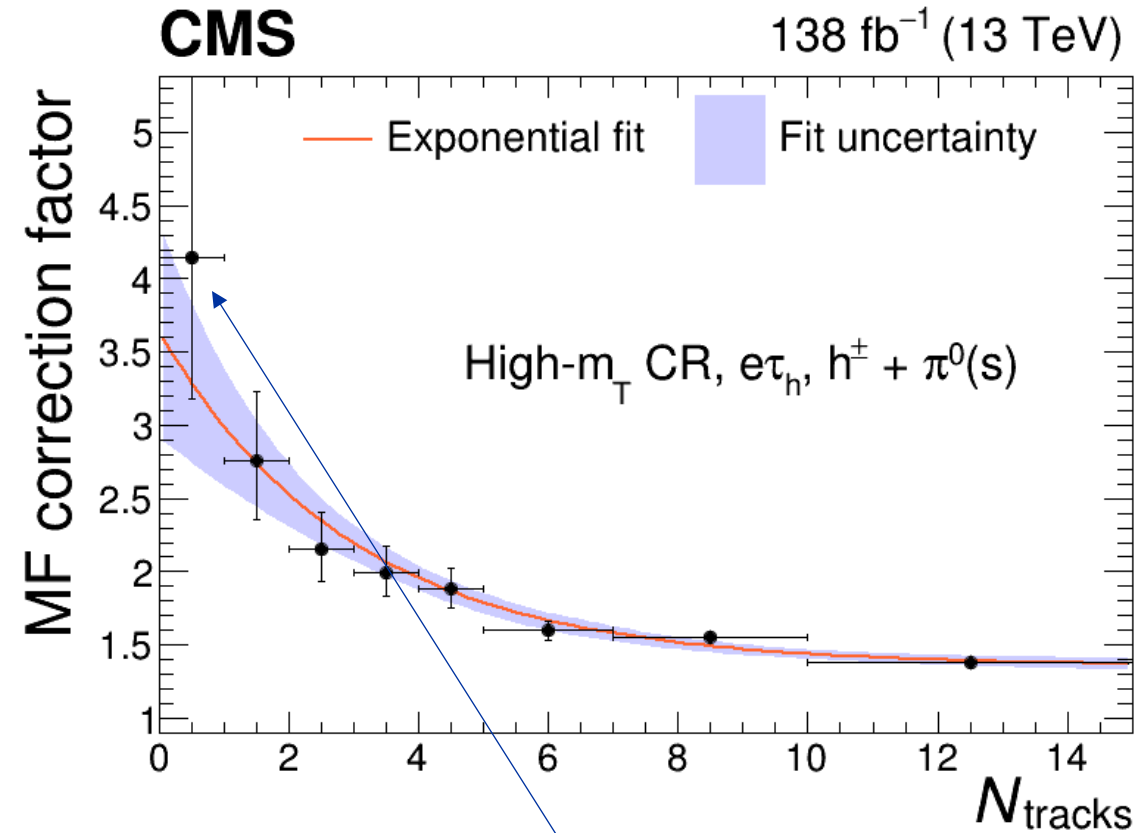
- In data control regions (e.g. require SS leptons/ τ_h to enrich in QCD multijet events)
- To estimate background in the SR, select events passing the SR selection except the τ_h fails the nominal τ_h ID and reweigh them with MF

But it is not that simple...

How does N_{tracks} affect MF?

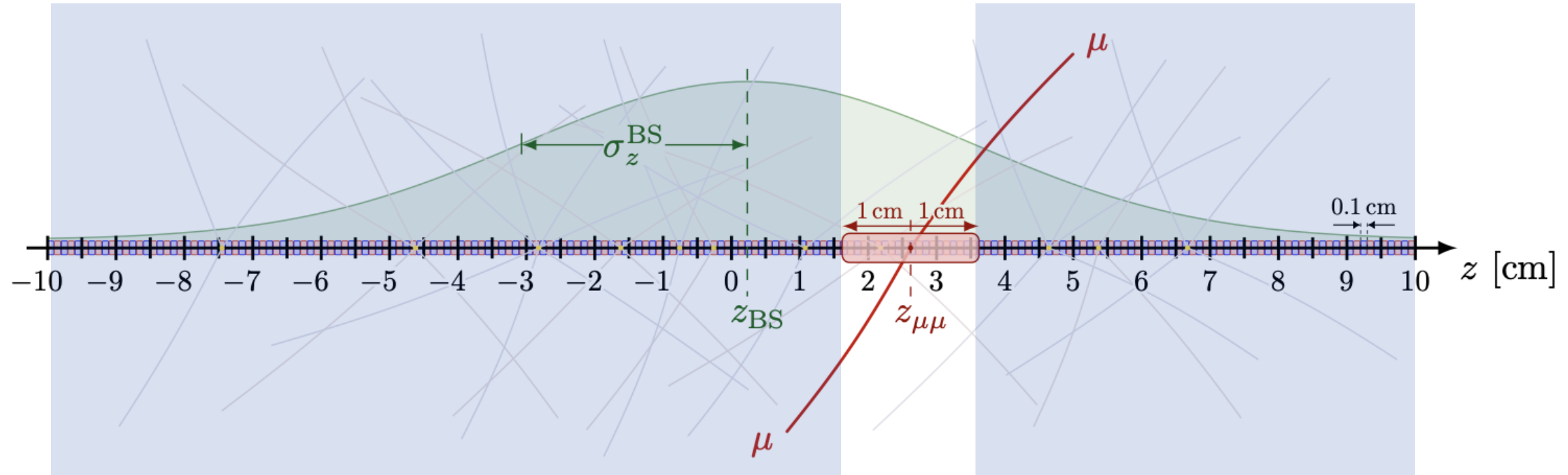
Jet $\rightarrow \tau_h$ mis-ID background (2)

- If there is less track activity around the τ_h candidate:
 - The τ_h candidate is more isolated
 - It is more likely to pass the ID criteria
 - MF is higher
- Model N_{tracks} dependence with a multiplicative correction to the mis-ID rates
 - Parameterized with exponential at low N_{tracks}



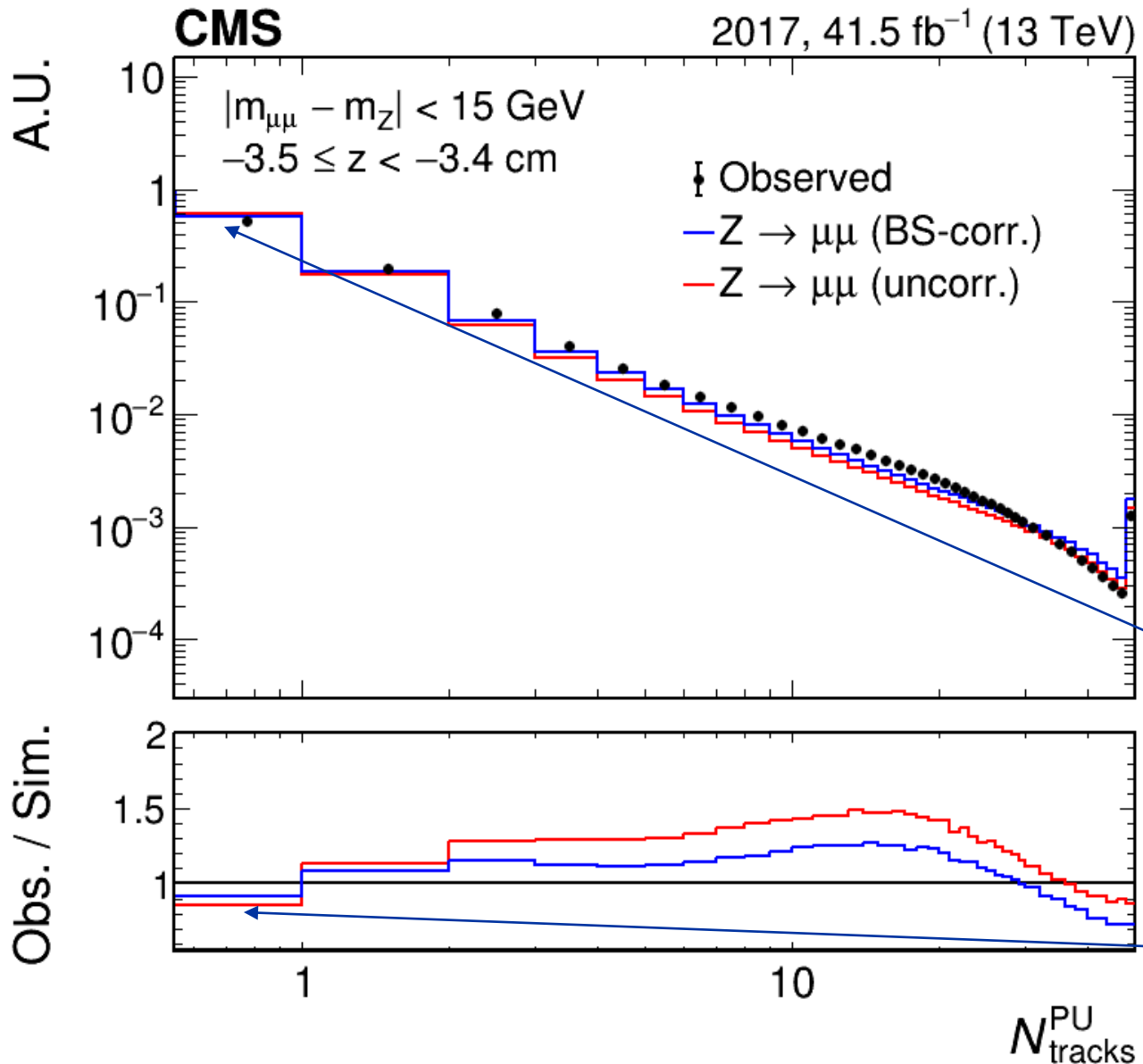
The jet is 4 times more likely to pass the nominal τ_h ID criteria if there is no other track at the vertex

Pileup track multiplicity correction



- Can simulations describe accurately the number of pileup tracks within windows of 0.1 cm width all over the z axis?
- Compare N_{tracks} distribution in $Z \rightarrow \mu\mu$ data and $Z \rightarrow \mu\mu$ MC, inside windows sampled over the z axis far ($> 1\text{cm}$) from the $\mu\mu$ vertex

Pileup track multiplicity correction

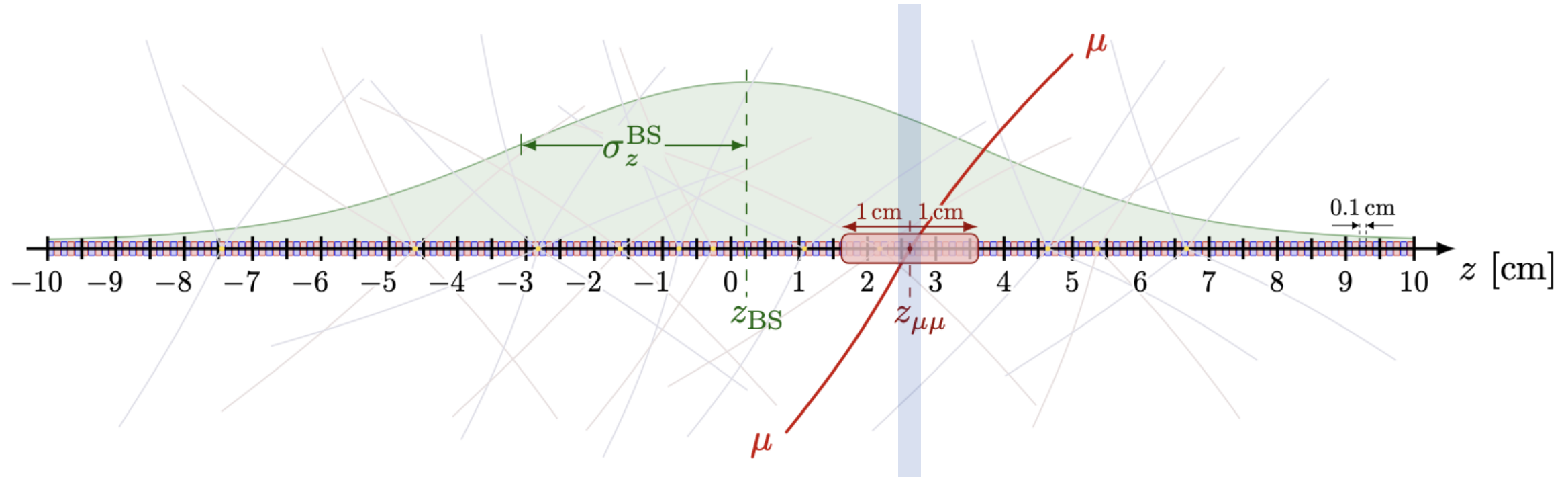


- Correction derived as a function of N_{tracks} and z

1 beamspot width away from beamspot center,
50% of windows do not contain any PU track

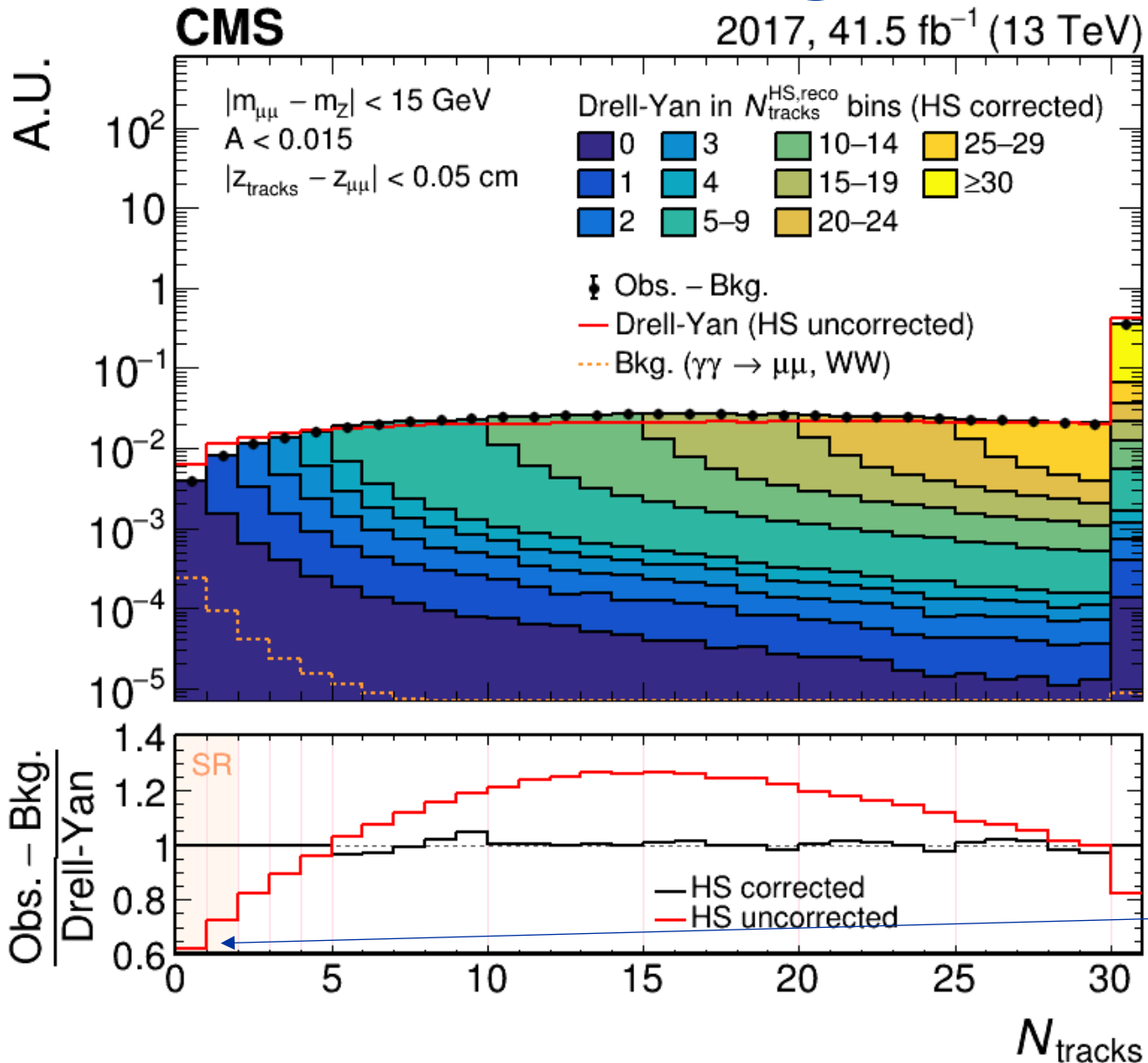
For a window 1 beamspot width away from
beamspot center with no PU track inside, the
event-weight correction is 0.95

Hard scattering track multiplicity correction



- Can the Drell-Yan simulation describe accurately the number of tracks from the hard interaction in windows of 0.1 cm width?
- Compare N_{tracks} distribution in $Z \rightarrow \mu\mu$ data and $Z \rightarrow \mu\mu$ MC (subtracting elastic processes), inside window centered at the $\mu\mu$ vertex

Hard scattering track multiplicity correction

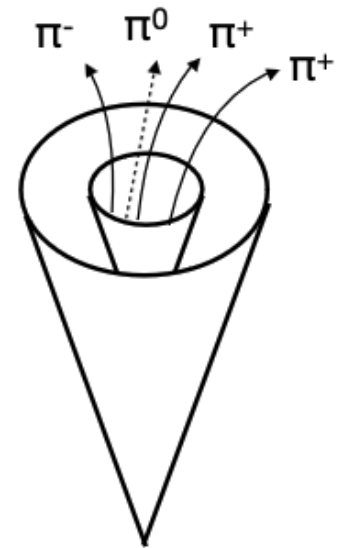


- Compare number of reconstructed tracks in data and in DY simulation at the $\mu\mu$ vertex
- These tracks can come from pileup or from the hard interaction
- Split simulation based on the number of reconstructed tracks associated to the hard interaction, and rescale all components simultaneously to match the data

Simulated Drell-Yan events with no reconstructed track associated to the hard interaction in the $\mu\mu$ window should be assigned a weight of ~ 0.6

Interlude: τ decay and reconstruction

- **Leptonic τ decays (~35%):** 1 electron or 1 muon + 2 neutrinos
 - Reconstructed as standard electrons and muons
- **Hadronic τ decays (τ_h , ~65%):** 1 or 3 charged hadrons + sometimes p0s + 1 neutrino
 - Reconstructed as 1 or 3 tracks with energy deposits in the calorimeters
- Always missing energy in the detector from escaping neutrinos



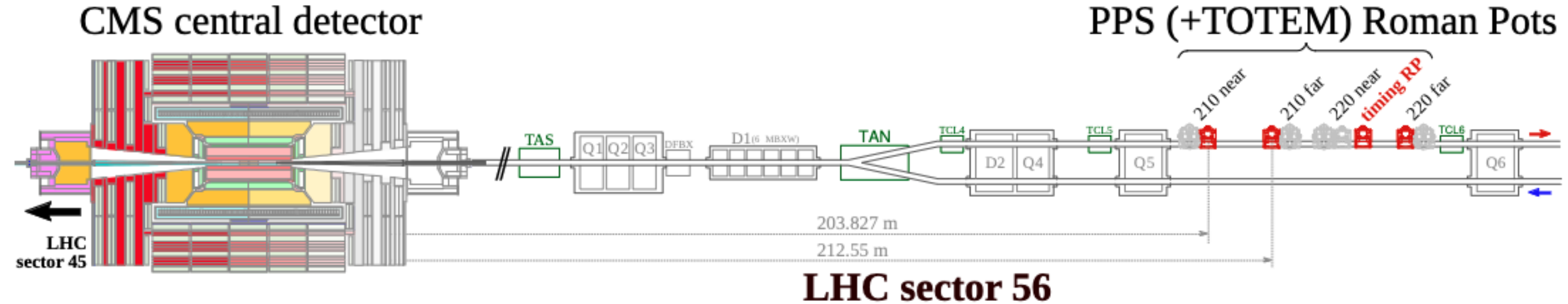
| Decay mode | Meson resonance | \mathcal{B} [%] |
|---|-----------------|-------------------|
| $\tau^- \rightarrow e^- \bar{\nu}_e \nu_\tau$ | | 17.8 |
| $\tau^- \rightarrow \mu^- \bar{\nu}_\mu \nu_\tau$ | | 17.4 |
| $\tau^- \rightarrow h^- \nu_\tau$ | | 11.5 |
| $\tau^- \rightarrow h^- \pi^0 \nu_\tau$ | $\rho(770)$ | 26.0 |
| $\tau^- \rightarrow h^- \pi^0 \pi^0 \nu_\tau$ | $a_1(1260)$ | 9.5 |
| $\tau^- \rightarrow h^- h^+ h^- \nu_\tau$ | $a_1(1260)$ | 9.8 |
| $\tau^- \rightarrow h^- h^+ h^- \pi^0 \nu_\tau$ | | 4.8 |
| Other modes with hadrons | | 3.2 |
| All modes containing hadrons | | 64.8 |

**1 prong
~47%**

**3 prongs
~15%**

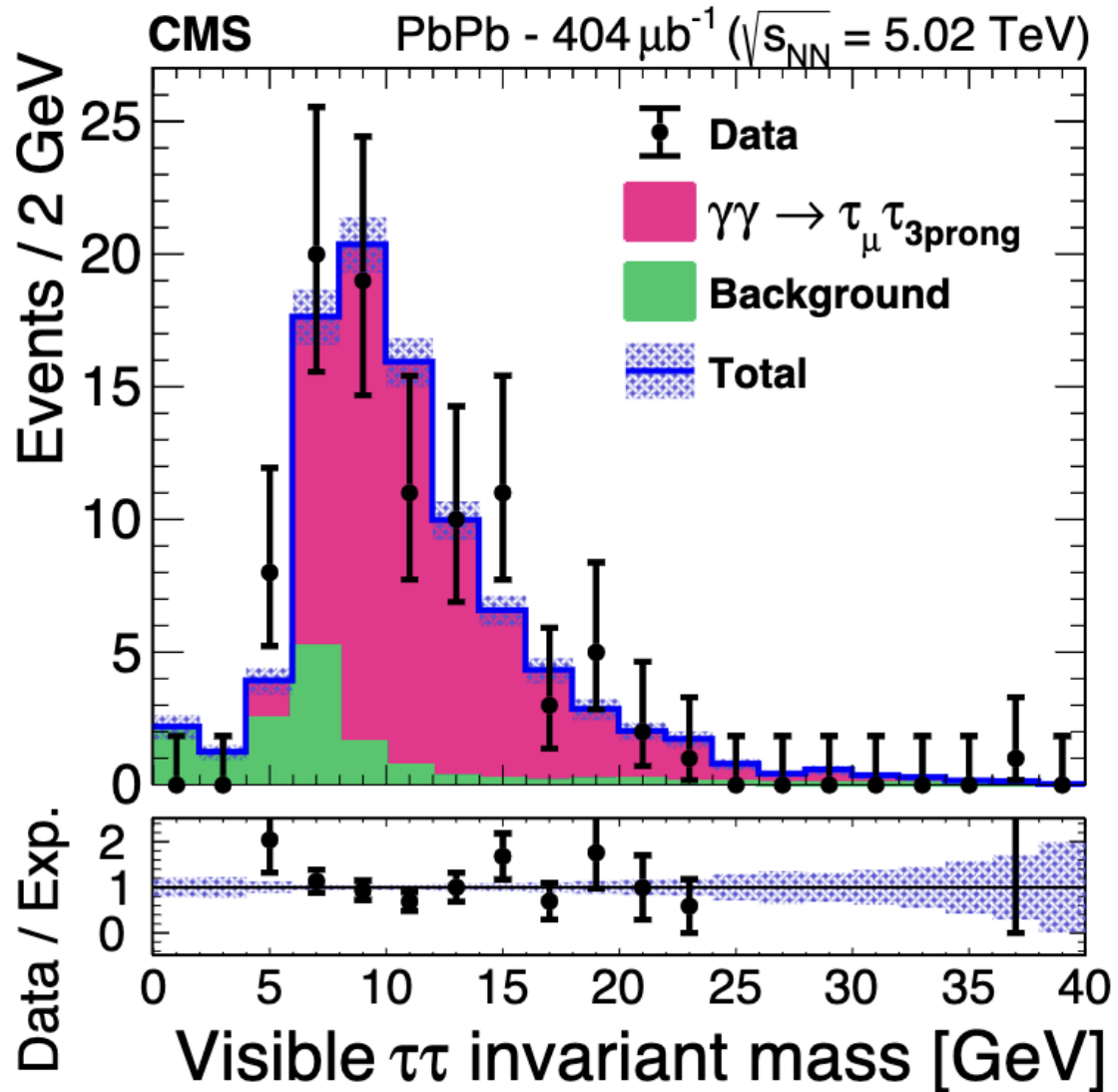
Analyses with τ leptons are difficult because of variety of possible decays, and large backgrounds mimicking τ signature

The high energy regime – pp collisions with proton tagging



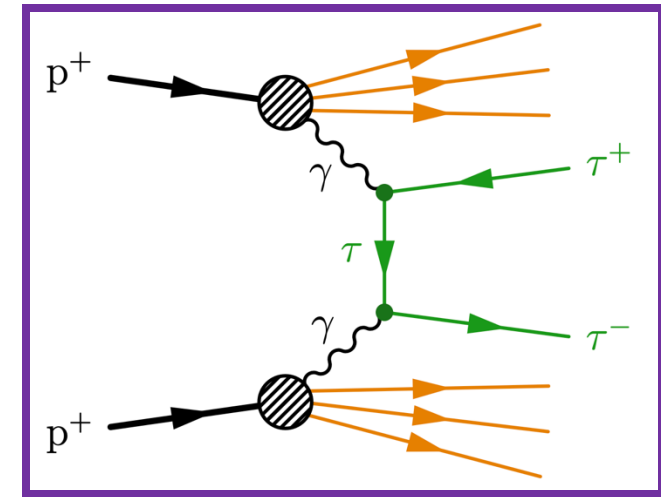
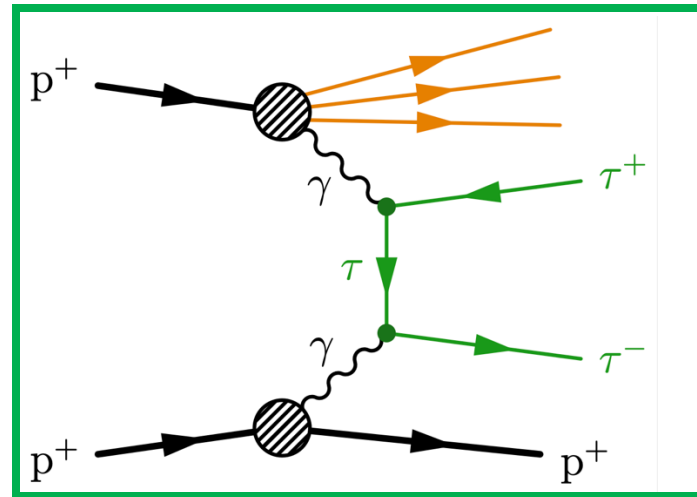
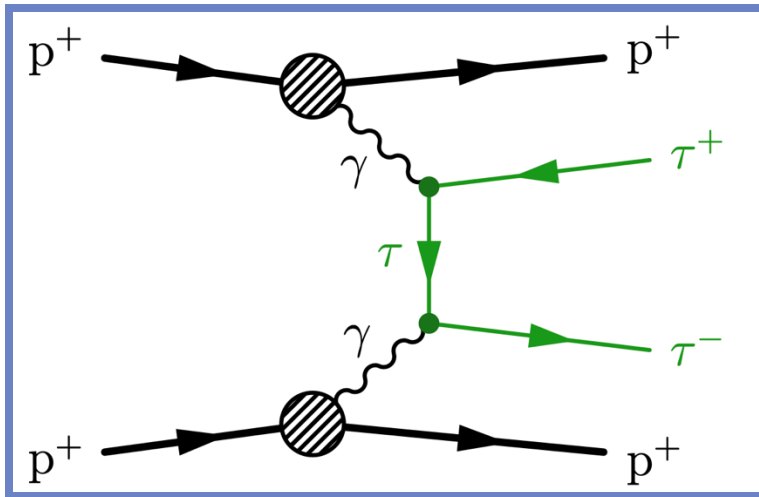
- PPS is a forward detector situated ~200 meters away from CMS (1 PPS arm on each side)
- Can tag diffracted protons that have lost a small fraction of their energy
- Proton kinematics (from PPS) correlated to kinematics of central system (from CMS) → powerful handle to reduce backgrounds

$\gamma\gamma \rightarrow \tau\tau$ in PbPb ultraperipheral collisions



- $\gamma\gamma \rightarrow \tau\tau$ observed recently in Pb-Pb collisions by both CMS and ATLAS
- Clean channel with small background contributions
- Accessing phase space with $m_{\tau\tau} \gtrsim 25 \text{ GeV}$

Including (semi-)dissociative contributions

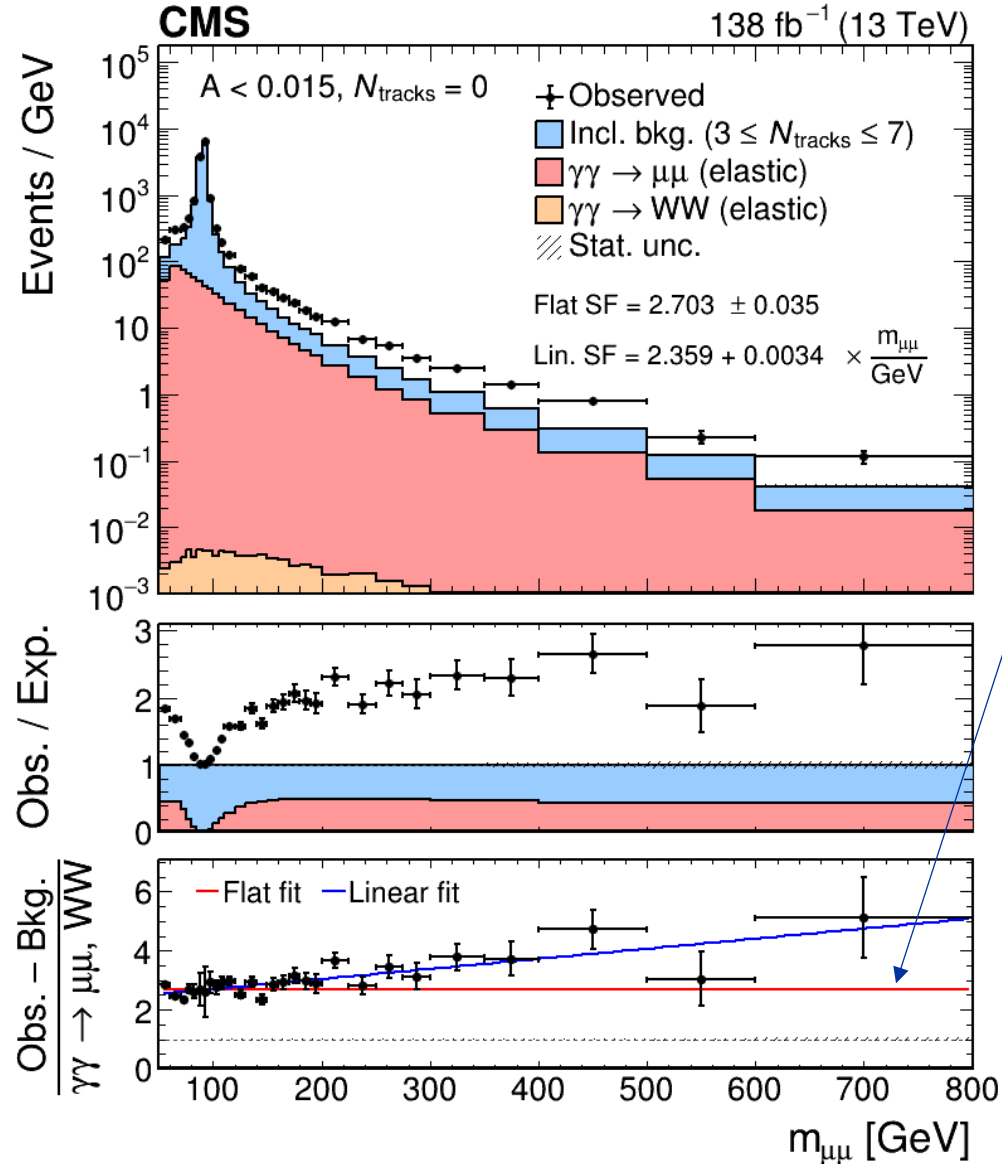


- **Elastic-elastic (ee)** signal process modeled with gammaUPC
- **Single-dissociative (sd)** and **double-dissociative (dd)** processes have larger cross section and may end up with an exclusive signature \rightarrow rescale elastic signal to include these contributions
- Scaling factor = $(ee + sd + dd)_{obs} / ee_{sim}$ can be measured with $\gamma\gamma \rightarrow \mu\mu$ in the $\mu\mu$ CR and applied to $\gamma\gamma \rightarrow ee/\mu\mu/\tau\tau/WW$ in the signal region

Including (semi-)dissociative contributions

- Elastic $\gamma\gamma \rightarrow \mu\mu / WW$:

- Estimated with gammaUPC
- Rescaled with linear $m_{\mu\mu}$ function to match data



Elastic simulation should be scaled by ~2.7 to describe all photon-induced contributions

Compatible with SuperChic predictions

Observation of $\gamma\gamma \rightarrow \tau\tau$

- 5.3 σ observed, 6.5 σ expected
- First observation of $\gamma\gamma \rightarrow \tau\tau$ in pp runs

| | Observed | Expected |
|----------------|--------------|--------------|
| $e\mu$ | 2.3 σ | 3.2 σ |
| $e\tau_h$ | 3.0 σ | 2.1 σ |
| $\mu\tau_h$ | 2.1 σ | 3.9 σ |
| $\tau_h\tau_h$ | 3.4 σ | 3.9 σ |
| Combined | 5.3 σ | 6.5 σ |

Leading systematics

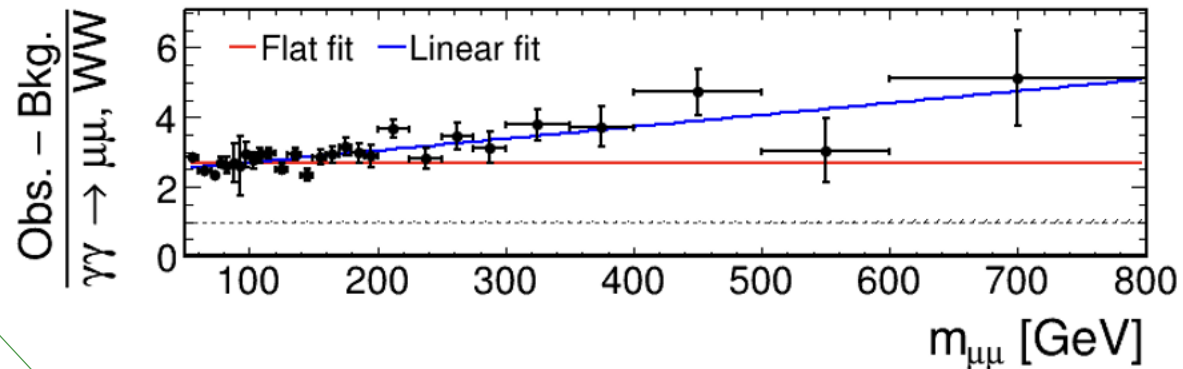
CMS

138 fb⁻¹ (13 TeV)

→ Fit ±1 σ impact

$$\hat{m} = 0.75^{+0.20}_{-0.18}$$

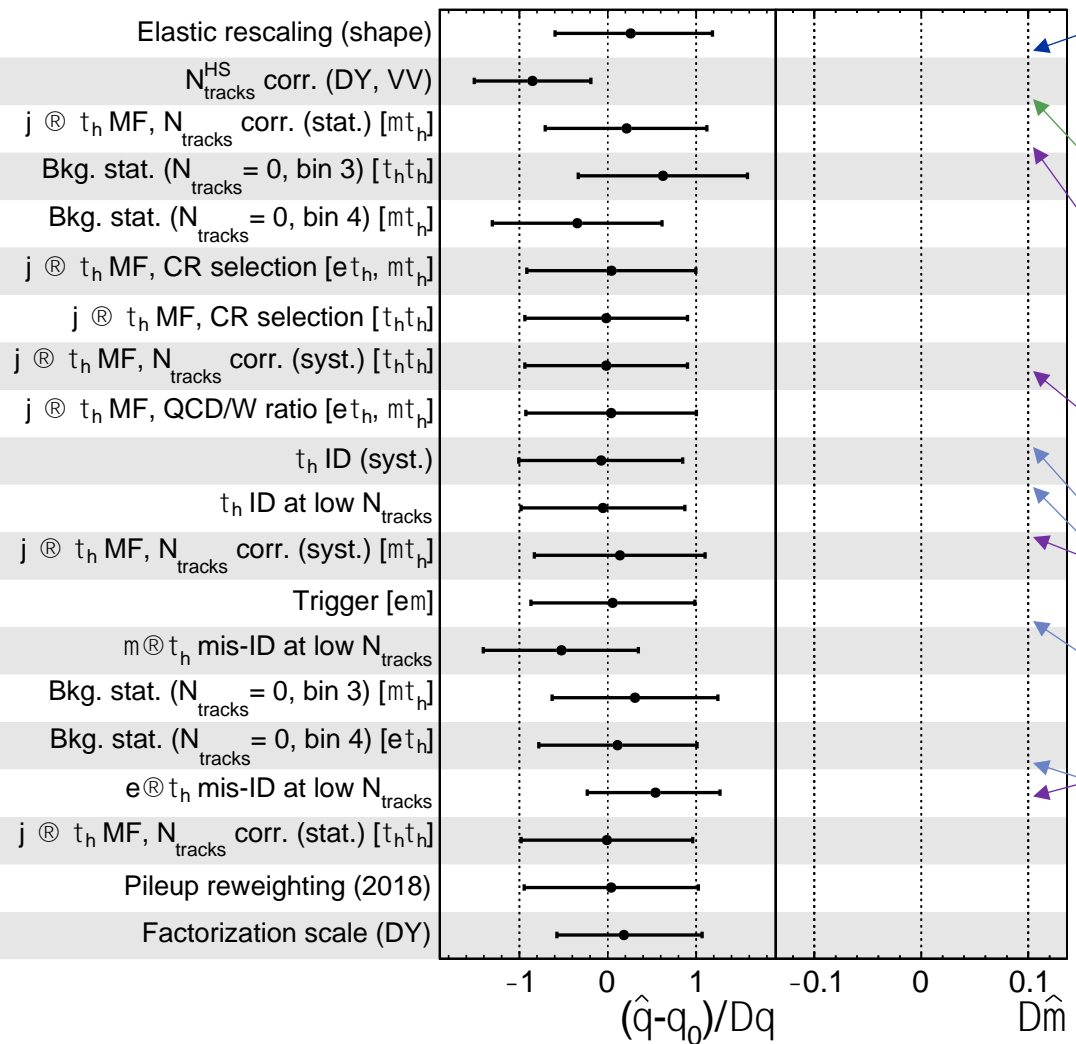
Considering the constant rescaling for the elastic simulations instead of the $m_{\mu\mu}$ -dependent one



UE/HS track multiplicity correction to Drell-Yan (6.5% uncertainty for $N_{\text{tracks}} = 0$)

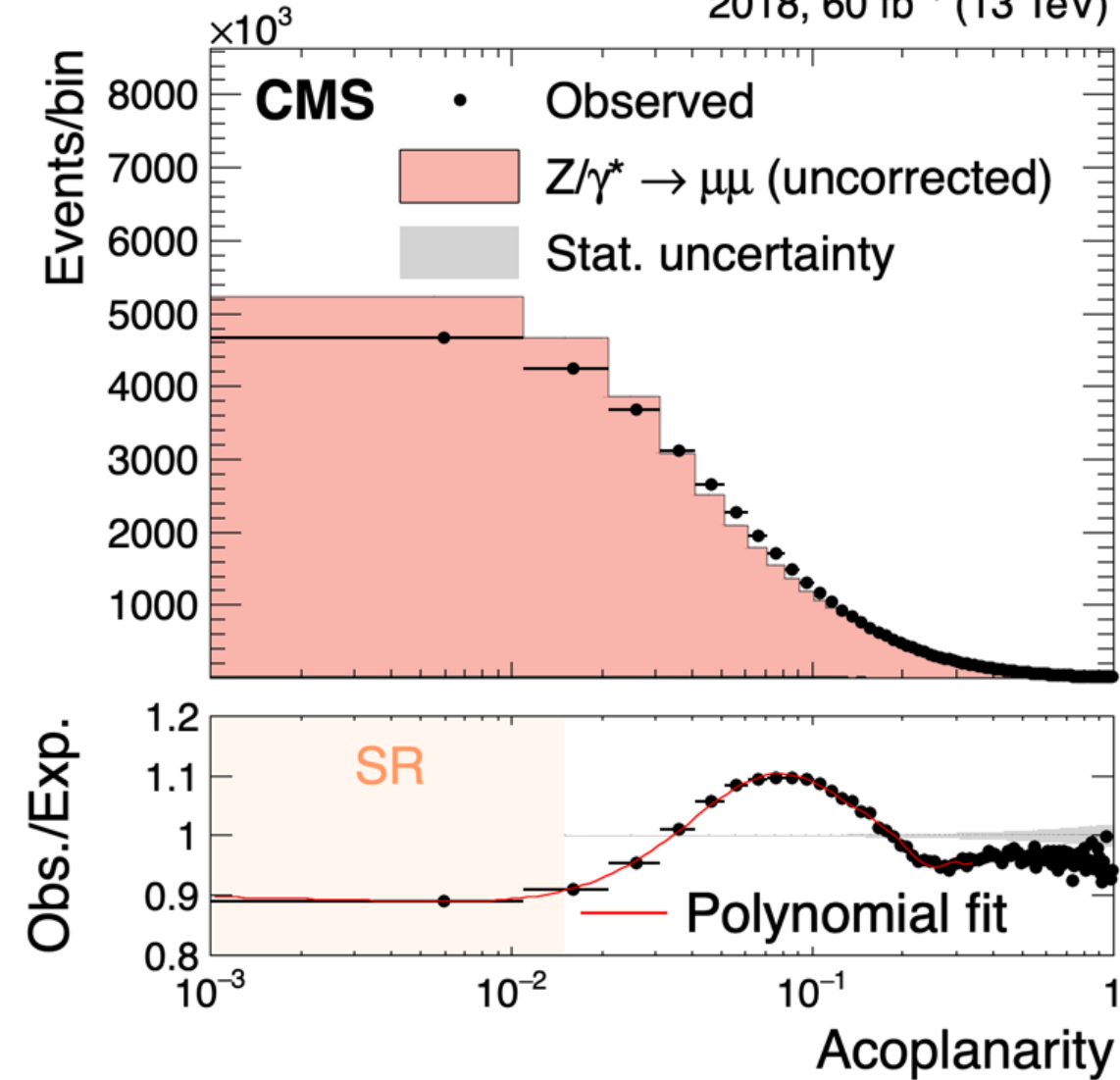
N_{tracks} extrapolation of the jet $\rightarrow \tau_h$ MF to estimate jet mis-ID background (up to ~20%)

Real and fake τ_h identification (at low N_{tracks})



Acoplanarity correction

2018, 60 fb⁻¹ (13 TeV)



- The Drell-Yan simulation does not model well the acoplanarity distribution in the dimuon control region
- Correction taken as Obs./Exp. Ratio in dimuon control region and applied in ditau signal region

$$A = 1 - \frac{|\Delta\phi|}{\pi}$$

Strategy

- In each of the 8 categories ($e\mu$, $e\tau_h$, $\mu\tau_h$, $\tau_h\tau_h$) \times ($N_{\text{tracks}} = 0$, $N_{\text{tracks}} = 1$), fit visible invariant mass of tau pair (m_{vis})
 - S/B ratio increases with m_{vis} because Drell-Yan background concentrated at lower masses and signal is nonresonant

Drell-Yan $Z/\gamma^* \rightarrow \tau\tau/ee/\mu\mu$

Resonant

From simulation

Jet $\rightarrow e/\mu/\tau_h$ mis-ID

Non-resonant

From data

Exclusive $\gamma\gamma \rightarrow ee/\mu\mu/WW$

Small but at low N_{tracks}

From elastic simulation

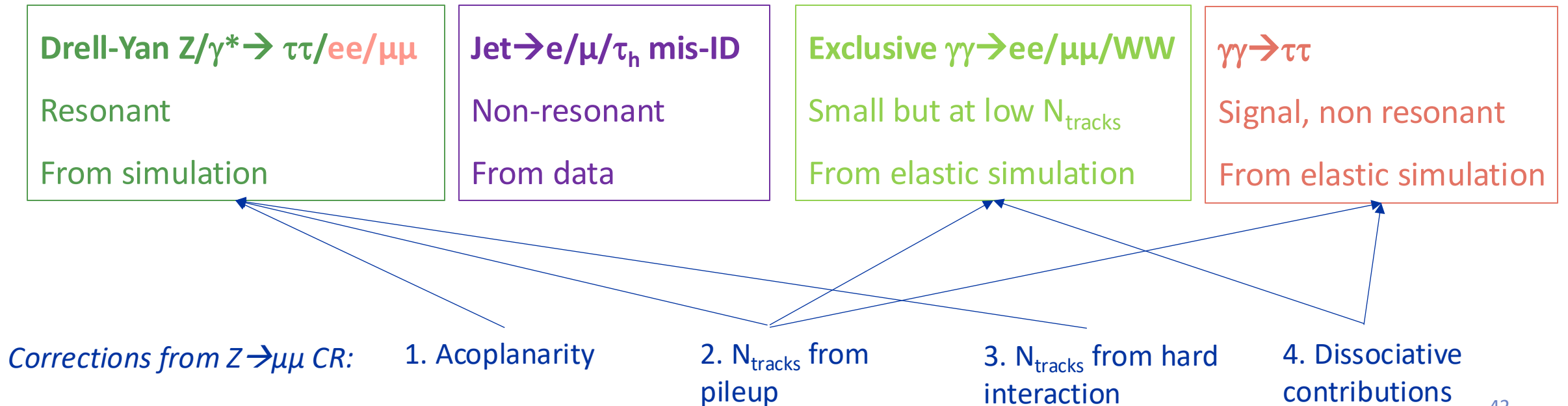
$\gamma\gamma \rightarrow \tau\tau$

Signal, non resonant

From elastic simulation

Strategy

- In each of the 8 categories $(e\mu, e\tau_h, \mu\tau_h, \tau_h\tau_h) \times (N_{\text{tracks}} = 0, N_{\text{tracks}} = 1)$, fit visible invariant mass of tau pair (m_{vis})
 - S/B ratio increases with m_{vis} because Drell-Yan background concentrated at lower masses and signal is nonresonant



Selection

Electron + muon triggers

Single lepton or lepton + τ_h triggers
 $p_T(\tau_h) > 30$ GeV to reduce fakes

| | $e\mu$ | $e\tau_h$ | $\mu\tau_h$ | $\tau_h\tau_h$ | $\mu\mu$ |
|---|-----------|---------------|---------------|----------------|----------------|
| p_T^e (GeV) | $> 15/24$ | $> 25 - 33$ | — | — | — |
| $ \eta^e $ | < 2.5 | $< 2.1 - 2.5$ | — | — | — |
| p_T^μ (GeV) | $> 24/15$ | — | $> 21 - 29$ | — | $> 26 - 29/10$ |
| $ \eta^\mu $ | < 2.4 | — | $< 2.1 - 2.4$ | — | — |
| $p_T^{\tau_h}$ (GeV) | — | $> 30 - 35$ | $> 30 - 32$ | > 40 | — |
| $ \eta^{\tau_h} $ | — | $< 2.1 - 2.3$ | $< 2.1 - 2.3$ | < 2.1 | — |
| $m_{\mu\mu}$ (GeV) | — | — | — | — | > 50 |
| OS | yes | yes | yes | yes | yes |
| $ d_z(\ell, \ell') $ (cm) | < 0.1 | < 0.1 | < 0.1 | < 0.1 | < 0.1 |
| $\Delta R(\ell, \ell')$ | > 0.5 | > 0.5 | > 0.5 | > 0.5 | > 0.5 |
| $m_T(e/\mu, \vec{p}_T^{\text{miss}})$ (GeV) | — | < 75 | < 75 | — | — |

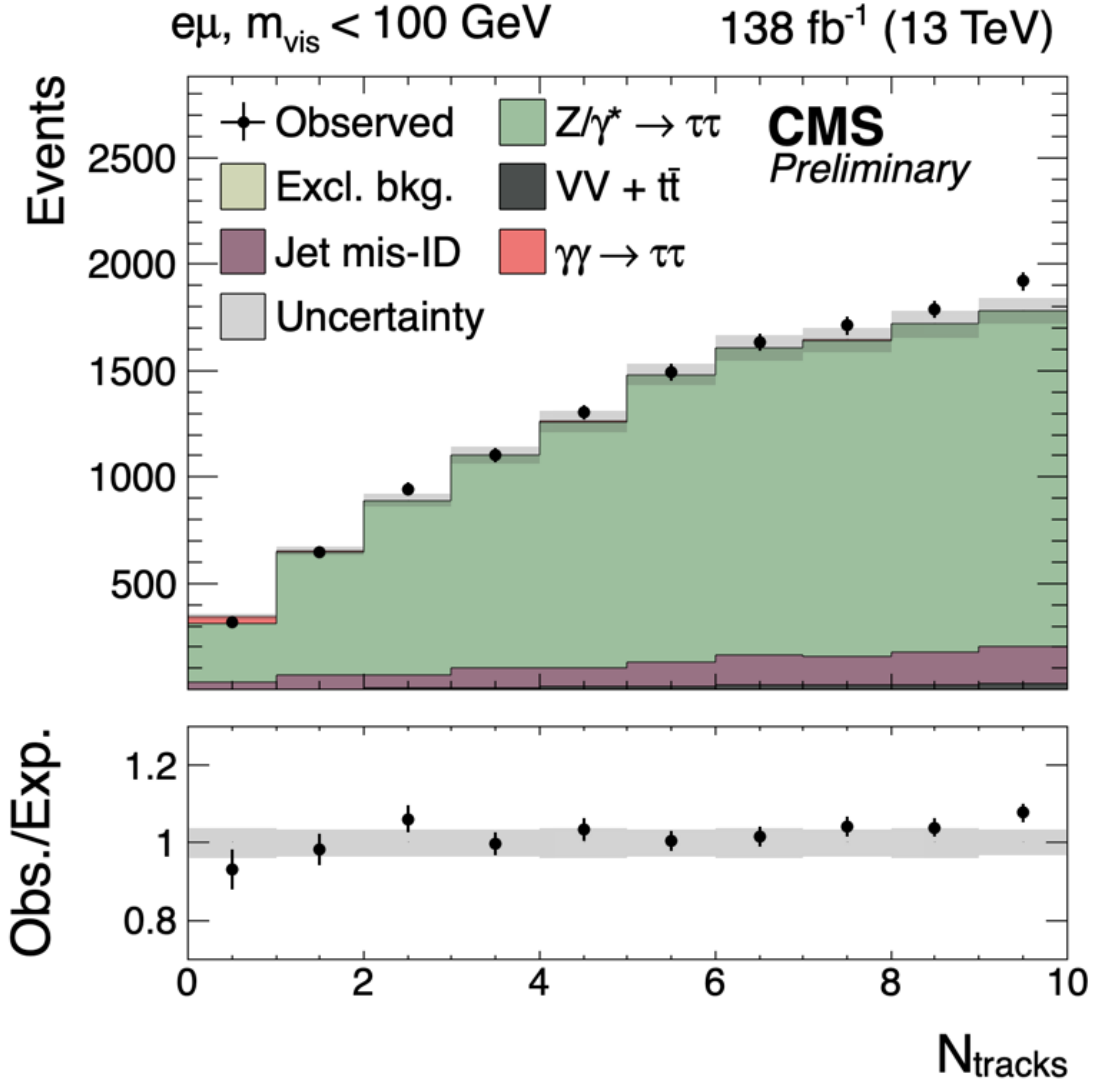
Di-tau trigger

To reduce
W+jets
background

In the signal regions, also require $A = 1 - \frac{|\Delta\phi|}{\pi} < 0.015$ and $N_{\text{tracks}} = 0$ or 1

Applying these corrections to $Z/\gamma^* \rightarrow \tau\tau$ simulation

- Good data/MC agreement in N_{tracks} distribution in all di-tau final states for the **DY-enriched** region with $m_{\text{vis}}(\tau, \tau) < 100 \text{ GeV}$



Limits on Wilson coefficients

